

PB-269 339

Critical Experiments, Measurements, and Analyses
to Establish a Crack Arrest Methodology for
Nuclear Pressure Vessel Steels

Battelle Columbus Labs., Ohio

Prepared for

Nuclear Regulatory Commission, Washington, D.C. Division of Reactor Safety
Research

Jun 77

**CRITICAL EXPERIMENTS, MEASUREMENTS,
AND ANALYSES TO ESTABLISH
A CRACK ARREST METHODOLOGY
FOR NUCLEAR PRESSURE VESSEL STEELS**

**Ninth Quarterly Progress Report
October - December 1976**

**Battelle Columbus Laboratories
for
U. S. Nuclear Regulatory Commission**

REPRODUCED BY
**NATIONAL TECHNICAL
INFORMATION SERVICE**
U. S. DEPARTMENT OF COMMERCE
SPRINGFIELD, VA. 22161

This report was prepared as an account of work sponsored by the United States Government. Neither the United States nor the United States Nuclear Regulatory Commission, nor any of their employees, nor any of their contractors, subcontractors, or their employees, makes any warranty, express or implied, nor assumes any legal liability or responsibility for the accuracy, completeness or usefulness of any information, apparatus, product or process disclosed, nor represents that its use would not infringe privately owned rights.

Available from
National Technical Information Service
Springfield, Virginia 22161
Price: Printed Copy \$4.50 ; Microfiche \$3.00

The price of this document for requesters outside of the North American Continent can be obtained from the National Technical Information Service.

**CRITICAL EXPERIMENTS, MEASUREMENTS,
AND ANALYSES TO ESTABLISH
A CRACK ARREST METHODOLOGY
FOR NUCLEAR PRESSURE VESSEL STEELS**

**Ninth Quarterly Progress Report
October - December 1976**

P. C. Gehlen M. F. Kanninen
G. T. Hahn C. W. Marshall
R. G. Hoagland C. Popelar
A. R. Rosenfield

Manuscript Completed: April 1977
Date Published: July 1977

Battelle Columbus Laboratories
505 King Avenue
Columbus, OH 43201
BMI-NUREG-1970

Prepared for
Division of Reactor Safety Research
Office of Nuclear Regulatory Research
U. S. Nuclear Regulatory Commission
Under Contract No. AT(49-24)-0293

FOREWORD

This project is part of a larger, coordinated effort of four institutions designed to establish a rational crack arrest methodology for nuclear pressure vessels. The program involves Battelle's Columbus Laboratories, the University of Maryland, Materials Research Laboratory, and the University of Illinois, and is being supported by the U. S. Nuclear Regulatory Commission and the Electric Power Research Institute. The program is implementing recommendations of a PVRC/MPC Working Group on crack arrest and includes work on dynamic fracture mechanics analysis, measurements of crack arrest in a variety of systems using common experimental materials, and photoelastic studies of fast fracture and arrest.

ABSTRACT

A comparison between the BCL one-dimensional and two-dimensional dynamic fracture models was made using experimental crack propagation results from a transparent plastic as a basis for the comparison. Both models gave essentially the same results in good agreement with experiment with regard to the important features of the fracture events, e.g. length of crack jump, and the variation in the instantaneous stress intensity and crack velocity with crack tip position during propagation. Some difficulties in these calculations due to the viscoelastic properties of the plastic are discussed. The one-dimensional beam-on-elastic foundation model was modified slightly by replacing the generalized foundation with a Winkler foundation. This modification leads to improved agreement between predicted and measured elastic compliances in the DCB geometry but has only a small effect on the character of the calculated run-arrest event.

Three compact tension (CT) geometry specimens were cut from previously machined single-edge-notch (SEN) specimens. These specimens were provided with larger diameter loading pins with the aim of reducing the specimen-load system interaction which had a pronounced influence on the crack propagation events in the previous SEN experiments. The results from these specimens do indeed indicate a significant reduction in the total amount of externally supplied energy during propagation although it is still significant as measurements of specimen motion indicate. The fast fracture toughness, K_{Ic} , data based on crack velocity measurements agree very well with K_{Ic} data obtained from DCB experiments. In addition, extensive crack bifurcation was not observed even though the specimens were provided with modest (25%) side grooves.

The influence of externally supplied energy during crack propagation was examined in some detail. An approximate relation was derived to indicate the magnitude of the error introduced into K_{Ic} data obtained from the measurement of crack jump distance. This method of determining K_{Ic} is intended to replace the experimentally more difficult procedure which requires measurement of crack velocity. The analysis provides a useful guide for specifying the necessary test-fixture stiffness for minimizing energy exchange between the specimen and fixture during a fracture event.

TABLE OF CONTENTS

	<u>Page</u>
FOREWORD	i
ABSTRACT	ii
1. PROGRAM SUMMARY	1-1
1.1. Introduction	1-1
1.2. Summary of Progress	1-2
1.3. Publications	1-3
2. DYNAMIC FRACTURE MECHANICS ANALYSIS	2-1
2.1. Introduction	2-1
2.2. Comparison of Calculations with Measurements of Crack Propagation and Arrest in Wedge- Loaded Rectangular-DCB Specimens of Araldite B	2-1
2.3. Comparison of One- and Two-Dimensional Analysis	2-20
3. APPLICATION OF THE COMPACT TENSION SPECIMEN GEOMETRY TO CRACK ARREST MEASUREMENTS - PRELIMINARY RESULTS	3-1
3.1. Introduction	3-1
3.2. Experimental Results	3-1
4. SOURCES OF ERROR IN K_D MEASUREMENTS - EFFECT OF EXTERNALLY SUPPLIED ENERGY DURING PROPAGATION	4-1
5. REFERENCES	5-1
ERRATA	iv

1. PROGRAM SUMMARY

1.1. Introduction

This report describes the research performed in the ninth quarter -- 1 October to 31 December 1976 -- of a 3-year program on crack arrest. The program is aimed at a crack arrest methodology for heavy-walled pressure vessels and nuclear grades of steel. Part of the research is being devoted to the development of one- and two-dimensional, dynamic fracture mechanics analyses of crack arrest, initially of the events studied in the laboratory and ultimately those of structural interest. The analytical work is being led by M. F. Kanninen, together with P. C. Gehlen and C. Popelar. The experimental work is aimed at the validation of the analyses, the development of a crack arrest testing practice, and the establishment of a crack arrest data base for nuclear grades of steels. This phase of the work is being led by R. G. Hoagland, together with A. R. Rosenfield, C. W. Marschall and G. T. Hahn. Overall responsibility of the program rests with G. T. Hahn.

The program consists of four tasks:

Task 1. The objective of this task is the development of one- and two-dimensional dynamic finite difference analyses of test pieces and models of a pressure vessel. The basic analytical methods have been worked out and are described in the Second Annual Report (BMI-NUREG-1959). Work is now underway to extend the two-dimensional analysis to a cylindrical section under thermal stress.

Task 2. This task provided critical experiments to validate analyses and theory and is essentially complete.

Task 3. This task has the objective of developing a testing practice for measuring K_{Ia} , the crack arrest material property, of both unirradiated and irradiated steel samples. The feasibility of one practice, based on wedge-loading a rectangular DCB (double cantilever beam) test piece has already been demonstrated (BMI-NUREG 1959, 1976). This test piece requires deep side grooves to stabilize the crack path and to prevent large-scale crack branching. In view of unresolved

questions about the grooves, alternative geometries, the SEN (single-edge-notched) and CT specimens, are being studied. The introduction of these geometries has created new problems particularly with regard to testing machine stiffness. In addition, a method for substantially reducing the volume of test material (particularly irradiated material) needed to perform fracture toughness and crack arrest tests has been evaluated.

Task 4. The objective of this task is to establish a crack arrest property data base for A533 and A508 once an acceptable test practice is in hand.

1.2. Summary of Progress

The research performed in this quarter pertains to Tasks 1 and 3, and is summarized in the following paragraphs.

Task 1. Dynamic Fracture Mechanics Analysis. During this reporting period the fully dynamic one-dimensional, beam-like and two-dimensional fracture analyses were examined in greater detail. These analyses have been developed at Battelle for the purpose of interpreting the dynamic fracture toughness, K_{ID} , and K_{Im} in the experiments on nuclear PV steels. A direct comparison was made between the predictions of the one-dimensional and two-dimensional models for a set of DCB experiments on a transparent plastic, Araldite B, reported by J. F. Kalthoff, et al. at the ASIM Symposium on Fast Fracture and Crack Arrest held in Chicago in June, 1976. These experiments are useful because they provide a direct measure of the stress intensity associated with a running crack through an optical technique known as the method of caustics. With regard to the length of crack jump (from initiation to arrest) and the variation of stress intensity and crack velocity with crack length during propagation, the agreement between the two analyses was very good and both also agreed well with the experimental data. Some uncertainty in the calculation is introduced due to the strain rate sensitivity of the elastic properties of this material but the errors are probably small. In addition, the one-dimensional model was modified slightly by replacing the generalized foundation with a Winkler foundation through removal of the torsional resistances of the foundation elements. This modification improves

agreement between the calculated and measured elastic compliances of DCB geometries but has only a small effect on the character of a calculated run-arrest event.

Task 3. Standard Test Practice for Unirradiated Steels. Work to develop a useful crack-line loaded two-dimensional geometry is continuing. Previous work on single-edge-notch specimens increased our awareness of the need for stiffness in the loading system. In particular, the elastic strain energy stored in the loading pins due to bending and compression at the contact points between the wedge and pins is quite large. As a consequence, crack propagation does not occur under fixed grip conditions since a portion of this energy is supplied to the specimen. Three SEN specimens were modified to a slightly more compliant compact tension (CT) geometry and the diameter of the load pins was increased by 40 percent. Crack propagation tests on these specimens show a substantial reduction in specimen-load system interaction compared to the SEN experiments although the energy input to the specimen is still significant. K_D determinations based on crack velocity measurements agree very well with earlier measurements derived from DCB tests. However, the crack jump length gives a K_D value which is 20 to 30 percent smaller. An approximate analysis based on an energy balance and the predictions of the one-dimensional and two-dimensional dynamic fracture models shows that this discrepancy would be the result of an increase in energy of the specimen by about 50 percent during propagation. Furthermore, this analysis, when used as a guide in designing a loading system, indicates that if K_D derived simply from a measurement of crack propagation distance is to be accurate to 10 percent, the loading system must have a stiffness about 10 times that of the test specimen. These investigations are continuing and we are hopeful that a simple useful, and reliable method based on the CT geometry will be devised.

1.3. Publications

Additional information can be found in the reports of this program issued previously:

Eighth Quarterly Progress Report (Contract No. AT(49-24)-0293), BMI-1966, February, 1977.

Second Annual Progress Report (Task Agreement No. 62, Contract No. W-7405-eng-92), BMI-1959, October, 1976.

Sixth Quarterly Progress Report (Task Agreement No. 62, Contract No. W-7405-eng-92), BMI-1951, July, 1976.

Fifth Quarterly Progress Report (Task Agreement No. 62, Contract No. W-7405-eng-92), BMI-1944, March, 1976.

Fourth Quarterly Progress Report (Task Agreement No. 62, Contract No. W-7405-eng-92), BMI-1939, November, 1975.

First Annual Progress Report (Task Agreement No. 62, Contract No. W-7405-eng-92), BMI-1937, August, 1975.

Second Quarterly Progress Report (Task Agreement No. 62, Contract No. W-7405-eng-92), BMI-1934, May, 1975.

First Quarterly Progress Report (Task Agreement No. 62, Contract No. W-7405-eng-92), January, 1975.

Topical Report: R. G. Hoagland, M. F. Kanninen, A. R. Rosenfield, G. T. Hahn, "Rectangular-DCB Specimens for Fast Fracture and Crack Arrest Measurements", BMI-1933, December, 1974.

"Dynamic Analysis of Crack Propagation and Arrest in DCB Test Specimen", M. F. Kanninen, C. Popelar, and P. C. Gehlen, ASTM Symp. Fast Fracture and Crack Arrest, Chicago, June 1976, to be published.

"A Crack Arrest Measuring Procedure for K_{Im} , K_{ID} , and K_{Ia} Properties", R. G. Hoagland, A. R. Rosenfield, P. C. Gehlen, and G. T. Hahn, ASTM Symp. Fast Fracture and Crack Arrest, Chicago, June 1976, to be published.

"Fast Fracture Toughness of Steels", G. T. Hahn, R. G. Hoagland, and A. R. Rosenfield, Int. Conf. on Dynamic Fracture Toughness, London, July 1976, to be published.

"Crack Branching in A533B Steel" prepared for presentation at ICF-4, Waterloo, Canada (1977).

"Crack Arrest and its Relation to Propagating Crack Toughness, K_D ", submitted to Met. Trans.

The first step in the dynamic fracture analysis consisted of a one-dimensional model applicable only to beam-like specimens. To simulate fast fracture in two-dimensional specimens, such as SEN or CT, a two-dimensional analysis was developed (BMI-NUREG-1959, 1976). The two-dimensional model however requires larger amounts of computer time and whenever possible the one-dimensional analysis should be used. As a result several attempts have been made to refine the one-dimensional analysis (BMI-NUREG-1959, 1976). One further refinement, namely the removal of the torsional springs between the beam and foundation is discussed here.

A formal comparison between the one- and two-dimensional models in the case of a DCB specimen is also given. The excellent agreement between the two models and experiment further justifies the use of the more economical one-dimensional analysis with beam-like specimens.

2.2. Comparison of Calculations with Measurements of Crack Propagation and Arrest in Wedge-Loaded Rectangular-DCB Specimens of Araldite B

In the case of steels, the dynamic fracture energy R (or K_D) as a function of crack speed can be inferred from measurements of crack speed or crack length at arrest and the use of either the one- or two-dimensional analysis. In the case of Araldite B [Kalthoff, et al. (1976)], and Homalite-100 [Kobayashi, et al. (1975)], independent measurements of K_D versus crack speed have been inferred from optical measurements in the vicinity of the crack tip. The availability of this data provides a means of verifying the computer models and it is specifically for this reason that Araldite B has been modelled in the present study.

The dimensions and elastic properties of the specimens of the Araldite B wedge-loaded DCB specimens used by Kalthoff are summarized in Table 2.1.

The measured dynamic stress intensity factor as a function of crack speed obtained from a number of tests is shown in Figure 2.1.

Geometric Properties

Initial slot length, a_0	68 mm
DCB - beam height, H	63.5 mm
DCB - beam length, W	321 mm
DCB - beam thickness, B	10 mm
Distance from beam end to pin, f_1	16 mm
Pin diameter	25 mm

Elastic Properties

Static elastic modulus	3380 MN/m ²
Dynamic elastic modulus	3660 MN/m ²
Dilatational wave speed, C_1	2500 m/s
Bar wave speed, C_0	1770 m/s ^(a)
Static Poisson's Ratio	0.33
Dynamic Poisson's Ratio	0.39
K_{Ic}	0.79 ± 0.13 MNm ^{-3/2} ^(b)

-
- (a) Calculated from the dilatational wave speed and the dynamic Poisson's Ratio.
- (b) Determined from the usual static K_{Ic} test.
- (c) Extrapolated from K_{ID} measurements as the crack speed tends to zero.

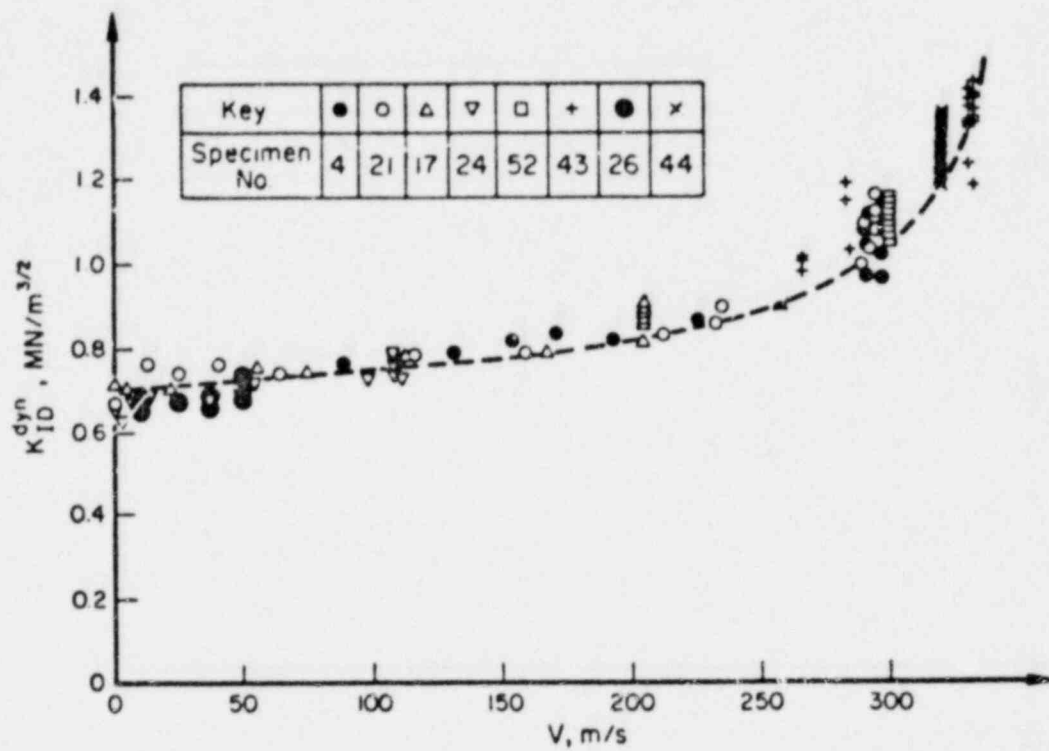


FIGURE 2.1. DYNAMIC STRESS INTENSITY FACTOR K_{ID} AS A FUNCTION OF CRACK VELOCITY V FOR ARALDITE B [Taken from Kalthoff (1976)]

the model in this study. The first one is related to the removal of the torsional springs between the beam and foundation and the second one is related to the usage of the static versus dynamic elastic properties in the analysis (see Table 2.1).

Firstly, in the development of the equations of motion for the DCB specimen (see page 2-4 of the First Annual Report, BMI-NUREG-1937, 1975) from the equations of motion of dynamic elasticity, the first equation of the latter was operated on by $\int_A z \, dydz$. After invoking the divergence theorem, which requires continuity of the stresses, one obtains a line integral

$$\int z (n_y \tau_{xy} + n_z \tau_{xz}) \, ds = k_r \delta \quad (2.1)$$

where the y and z axes are the principal centroidal axes and ds is the elemental arc length of the boundary of the cross section. The direction cosines of the unit normal to this boundary are denoted by n_y and n_z . Previously this integral was modeled by torsional foundation springs. However, a closer examination of this integral reveals that since the crack plane is a plane of symmetry ($\tau_{zy} = 0$, $n_y = 0$) and furthermore since the lateral surface of the DCB is stress free, then this integral and along with it the torsional stiffness of the foundation springs vanish.

The effect of the removal of the torsional springs is shown in Figure 2.2 for $K_Q = 1.34 \text{ MN/m}^{3/2}$. The crack growth versus time and energy versus crack growth curves are shown in Figure 2.3. From Figure 2.2 it is apparent that the computation with torsional springs (solid line) is overall somewhat closer to the experimental data (Δ) than the data obtained with a model without torsional springs (dotted line). However, the latter does reproduce the arrest length more accurately. In both computations the static elastic properties have been used throughout except in the relationship between K_D and crack speed (mixed elastic constants). The removal of the torsional springs lowered the initial strain energy from 0.188 to 0.144 joules. In the original computation the value of $K_Q = 1.34$ was used as input to compute a pin displacement, $\delta = 0.34 \text{ mm}$.

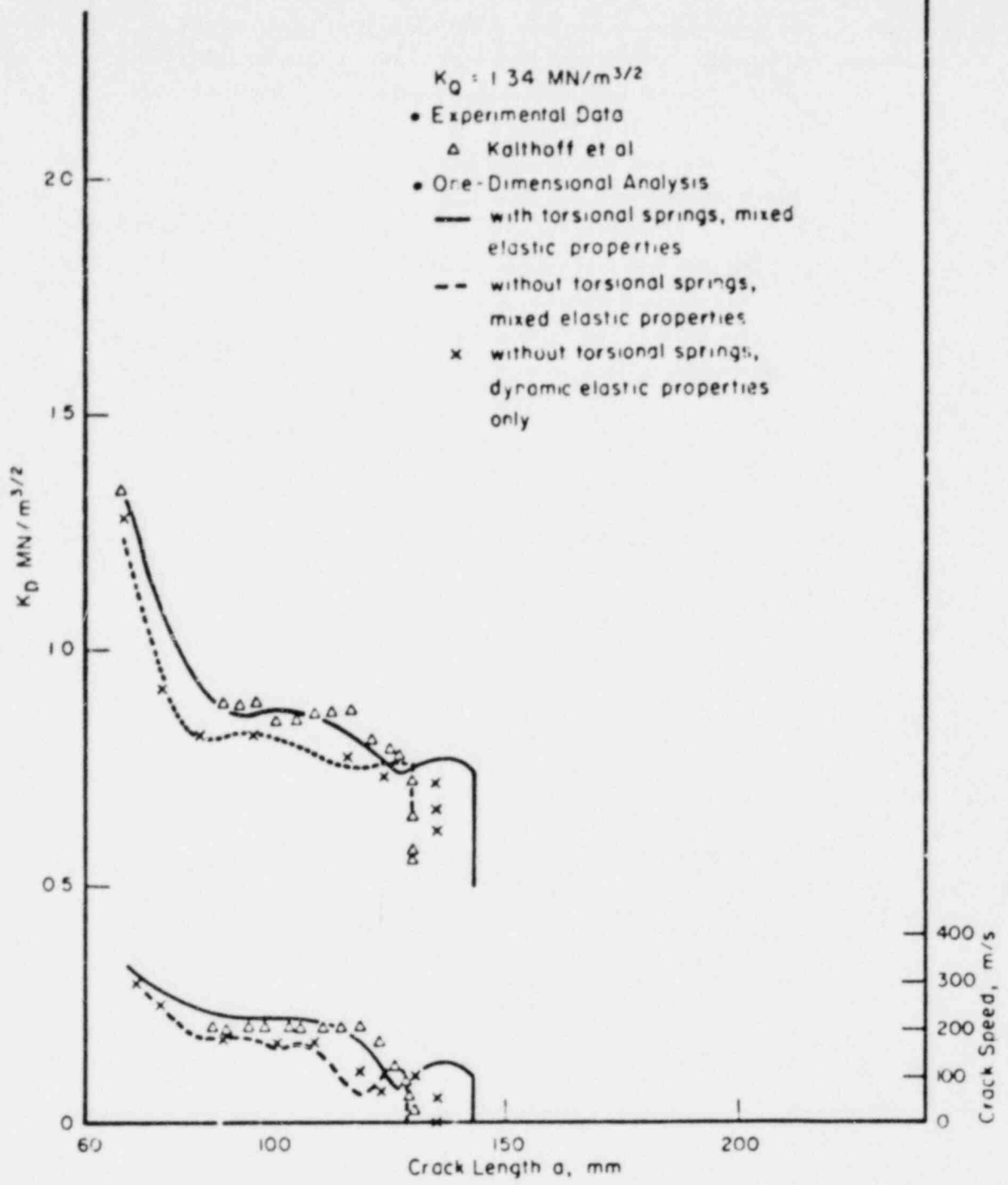
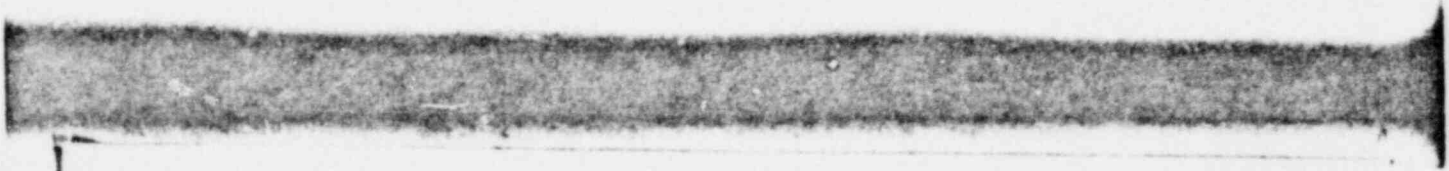


FIGURE 2.2. COMPARISON OF EXPERIMENTAL AND CALCULATED RESULTS FOR ARALDITE B



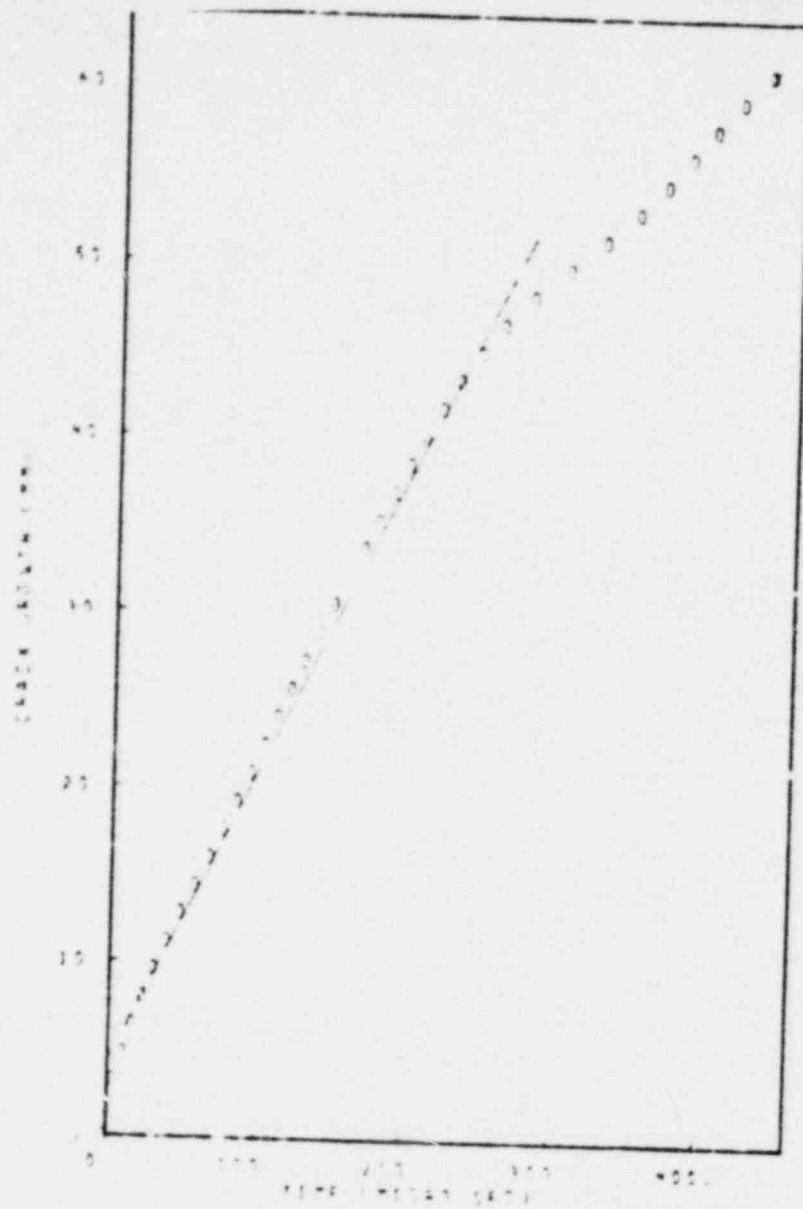
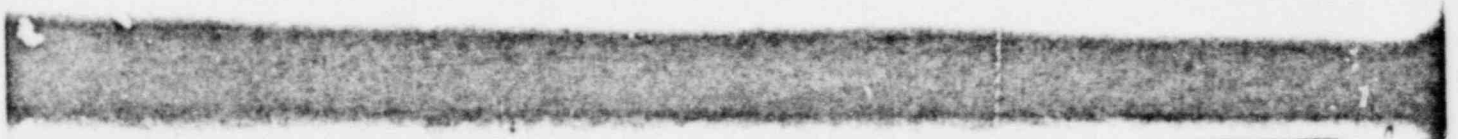


FIGURE 2.3. MODEL CALCULATION OF CRACK GROWTH AND ARREST VERSUS TIME IN WEDGE-LOADED RECTANGULAR DCB SPECIMENS OF ARALDITE B

a. Crack extension with time.



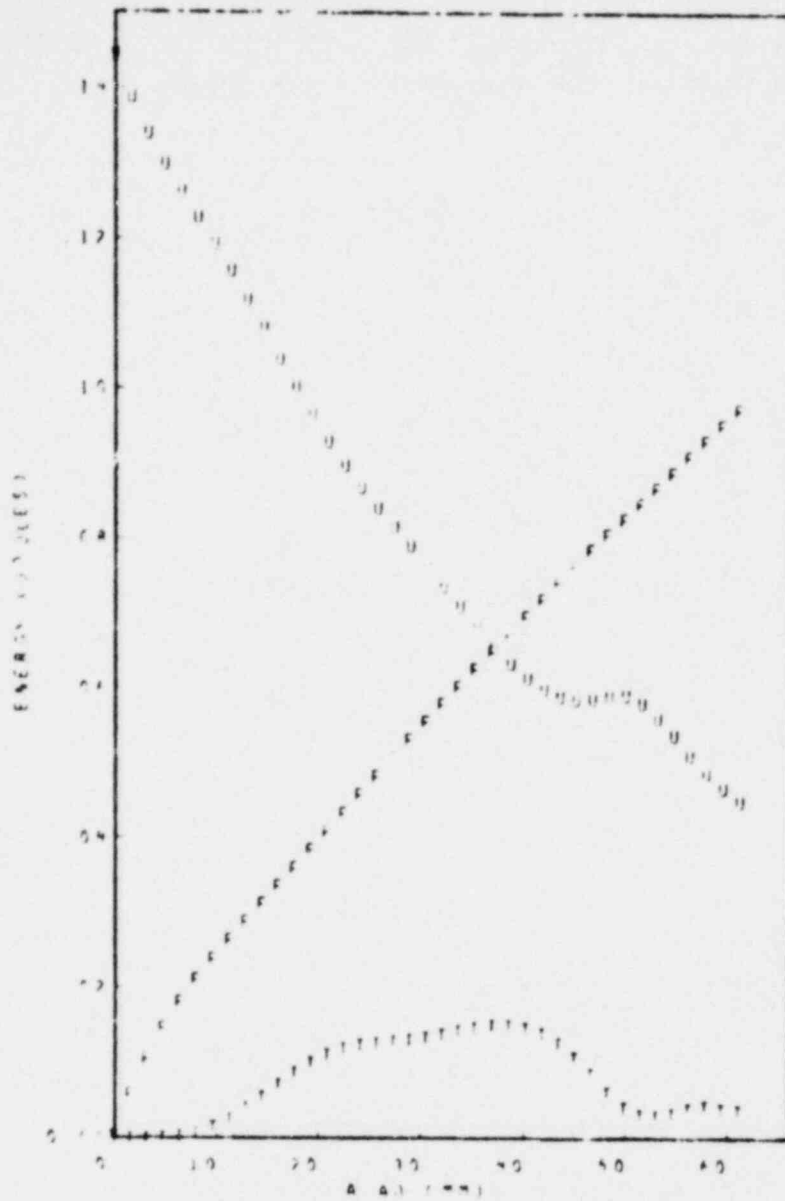


FIGURE 2.3. MODEL CALCULATION OF CRACK GROWTH AND ARREST VERSUS TIME IN WEDGE-LOADED RECTANGULAR DCB SPECIMENS OF ARALDITE B

b. Variation of strain (U), kinetic (T), and fracture (F) energies with crack extension. In this model the torsional springs were removed, the pin displacement was 0.34 mm and mixed elastic properties were used.

The removal of the springs will alter the relation between K_Q and δ . Since δ is the experimentally measured quantity, it was felt appropriate to keep it the same in the computation without torsional springs. The resulting value of K_Q was $1.24 \text{ MN/m}^{3/2}$. It may well be this lowering of K_Q and of the strain energy upon removal of the torsional springs causes the slight decrease in the K_D and velocity versus crack length data in Figure 2.2. It may also be for this reason that a shorter arrest length is predicted.

As pointed out above, the two model calculations described so far used both the static and dynamic elastic properties. Using the dynamic modulus only to relate K_D to R however leads to some inconsistencies in the computation, since our fracture criterion is based on a comparison of strain energy release rate \dot{W} (evaluated using a static modulus) to R (computed using the dynamic modulus). To remedy this inconsistency, the modulus used in the entire dynamic part of the model would have to be the dynamic one. This approach was tried for Homalite in EMI-NUREG-1933, 1974 and leads to rather poor agreement with experiment. There appears to be no unambiguous way to decide which elastic properties to use in which part of the model and at present it is probably safest to use the same elastic constants throughout the entire model. The axes (x) in Figure 2.2 show the results that were obtained when the dynamic modulus was used. As can readily be seen, these results and the ones generated with "mixed" elastic constants are in good agreement. Details of the crack growth versus time and energies versus crack growth curves for this case are shown in Figures 2.4a and b.

In addition to the results just discussed, Figure 2.5 shows similar data for $K_Q = 1.04$ and $K_Q = 2.35 \text{ MN/m}^{3/2}$. The corresponding crack growth versus time and energies versus crack growth are shown in Figure 2.5a-h.

Figure 2.5 shows that the previous results including torsional springs (solid line) and the results without torsional springs but using the dynamic elastic properties exclusively (---) bracket Kalthoff's experimental observations. Keeping in mind that the model neglects damping and that the error on the K_D versus crack speed relation may be as high as 15%, it is not possible to decide on the basis of Figure 2.5 which form of the model should be used. However, the model without torsional springs should be preferred on the following two grounds: 1) as pointed out

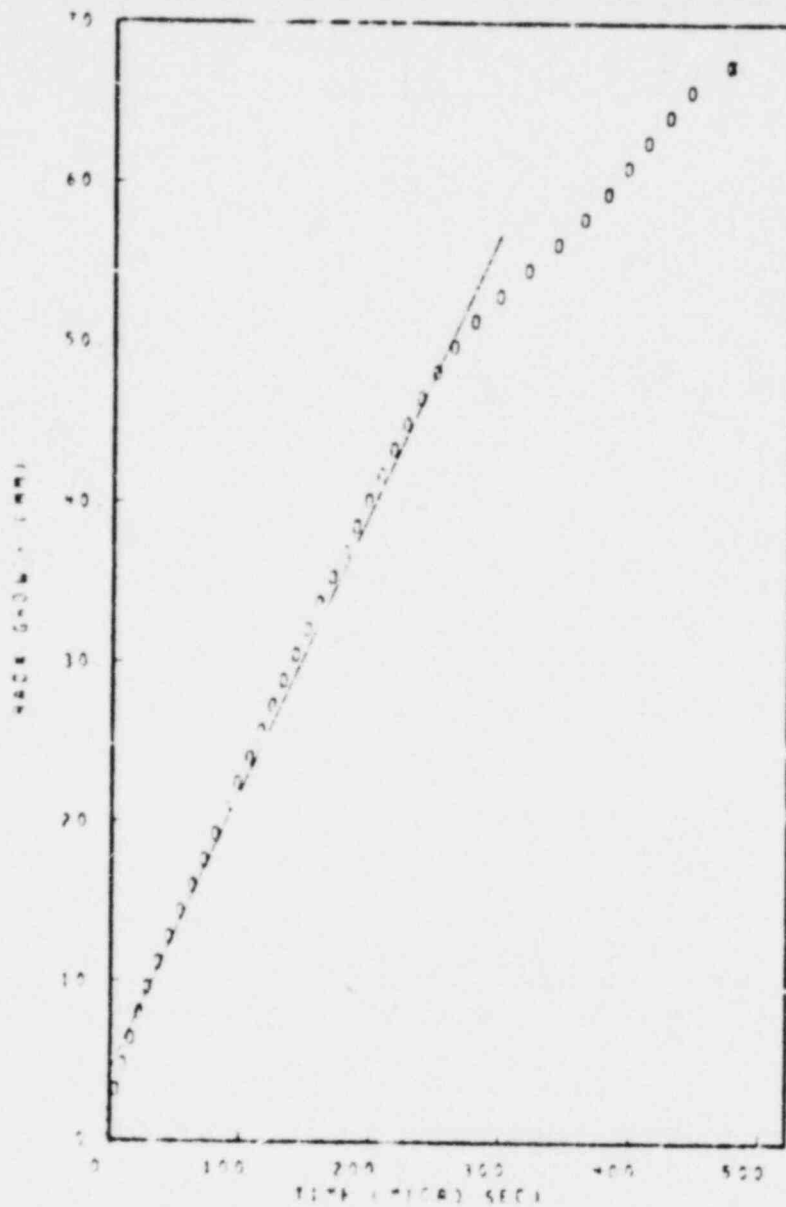


FIGURE 2.4. MODEL CALCULATION OF CRACK GROWTH AND ARREST IN WEDGE-LOADED RECTANGULAR DCB SPECIMEN OF ARALEDITE B

- a. In this model the torsional springs were removed, the pin displacement was 0.34 mm and dynamic elastic properties were used. Crack extension with time.

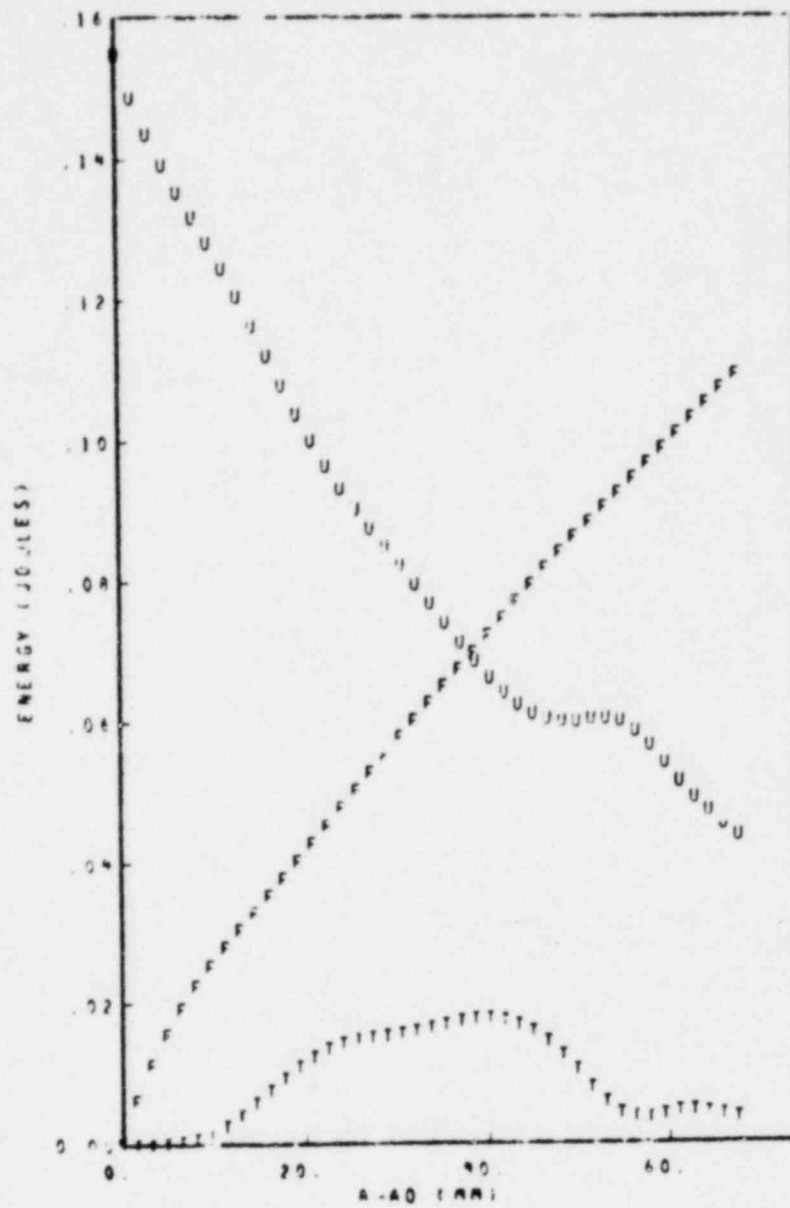


FIGURE 2.4. MODEL CALCULATIONS OF CRACK GROWTH AND ARREST IN WEDGE LOADED RECTANGULAR DCB SPECIMEN OF ARAIDITE B

b. Variation of strain (U), kinetic (T), and fracture (F) energies with crack extension.

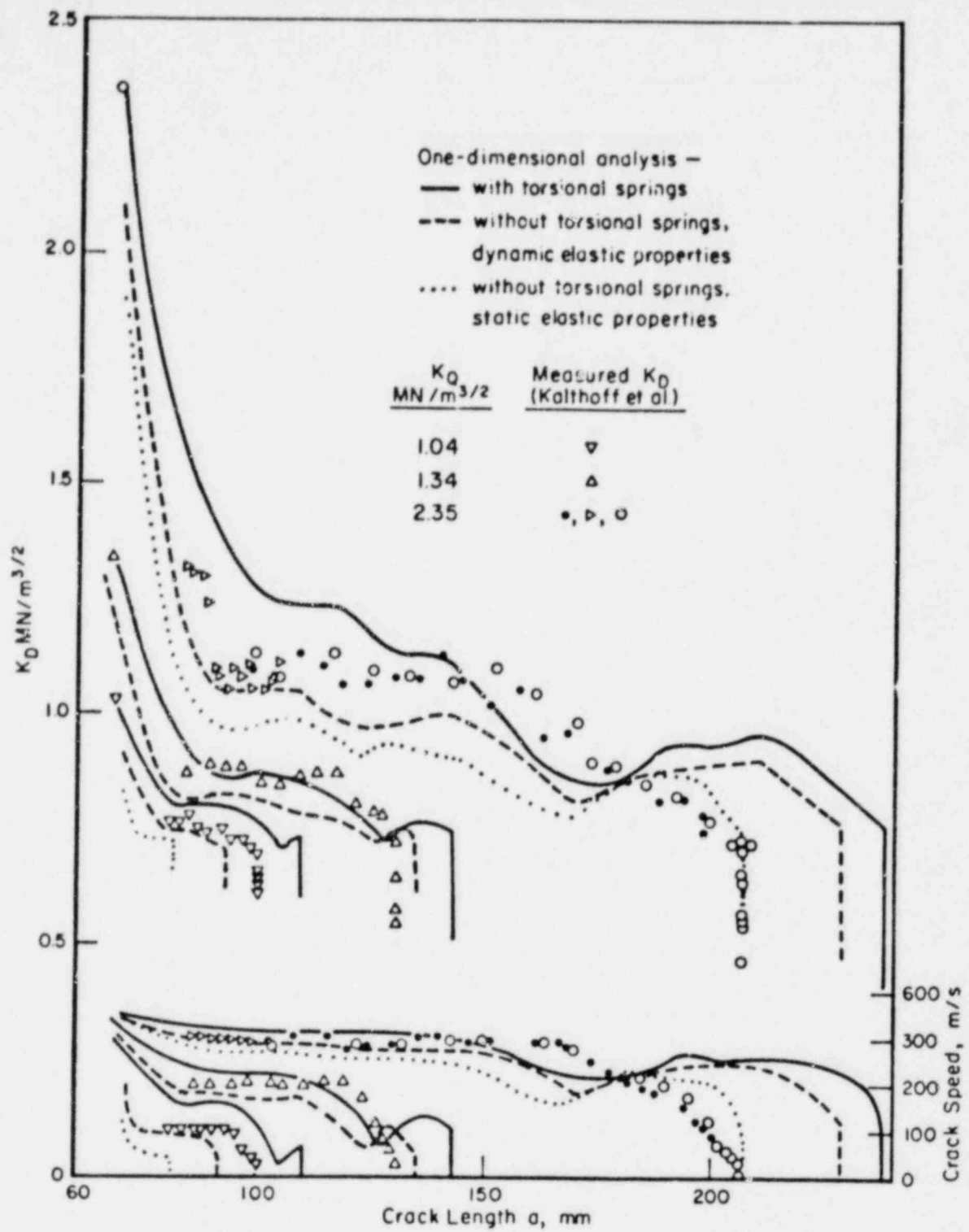


FIGURE 2.5. COMPARISON OF EXPERIMENTAL AND COMPUTED RESULTS FOR ARALDITE B

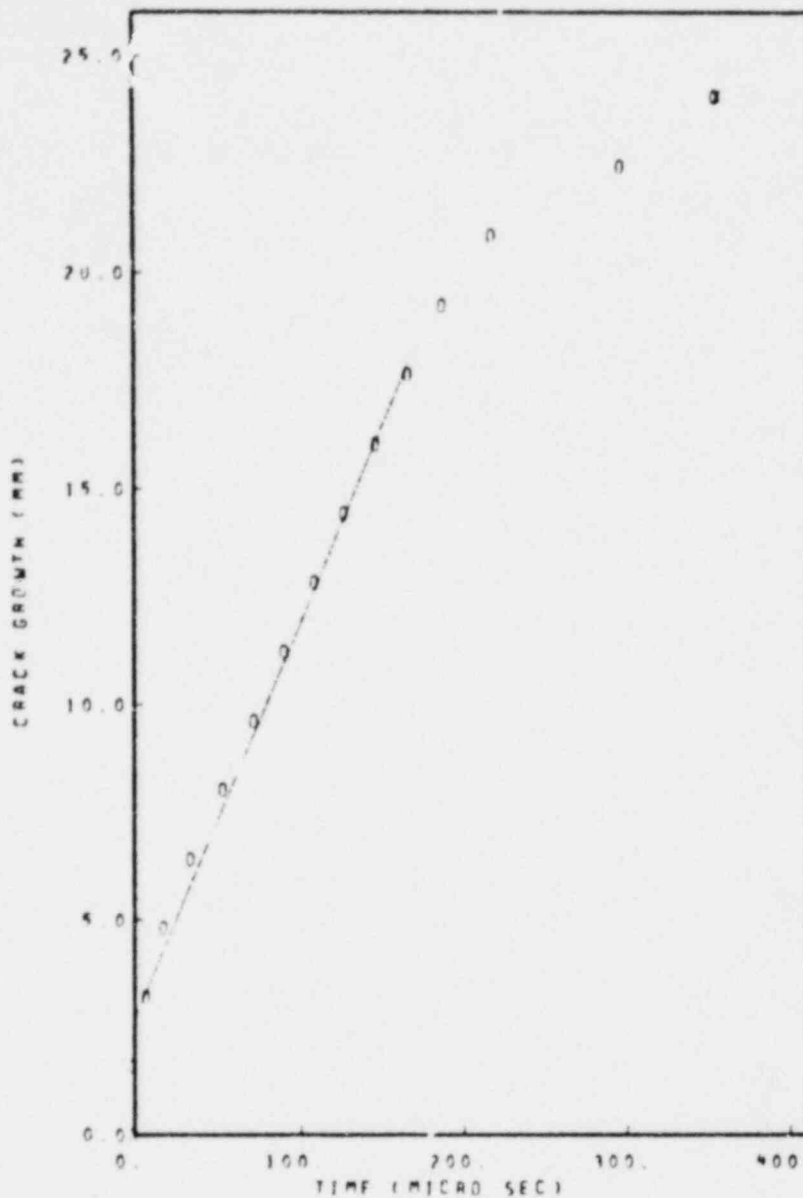


FIGURE 2.6. MODEL CALCULATIONS OF CRACK GROWTH VERSUS TIME AND ENERGIES VERSUS CRACK GROWTH IN WEDGE LOADED RECTANGULAR DCB SPECIMENS OF ARLDITE B

- a. $K_Q = 1.04$ (nominal), pin displacement 0.245 mm dynamic elastic properties used. Crack extension with time.

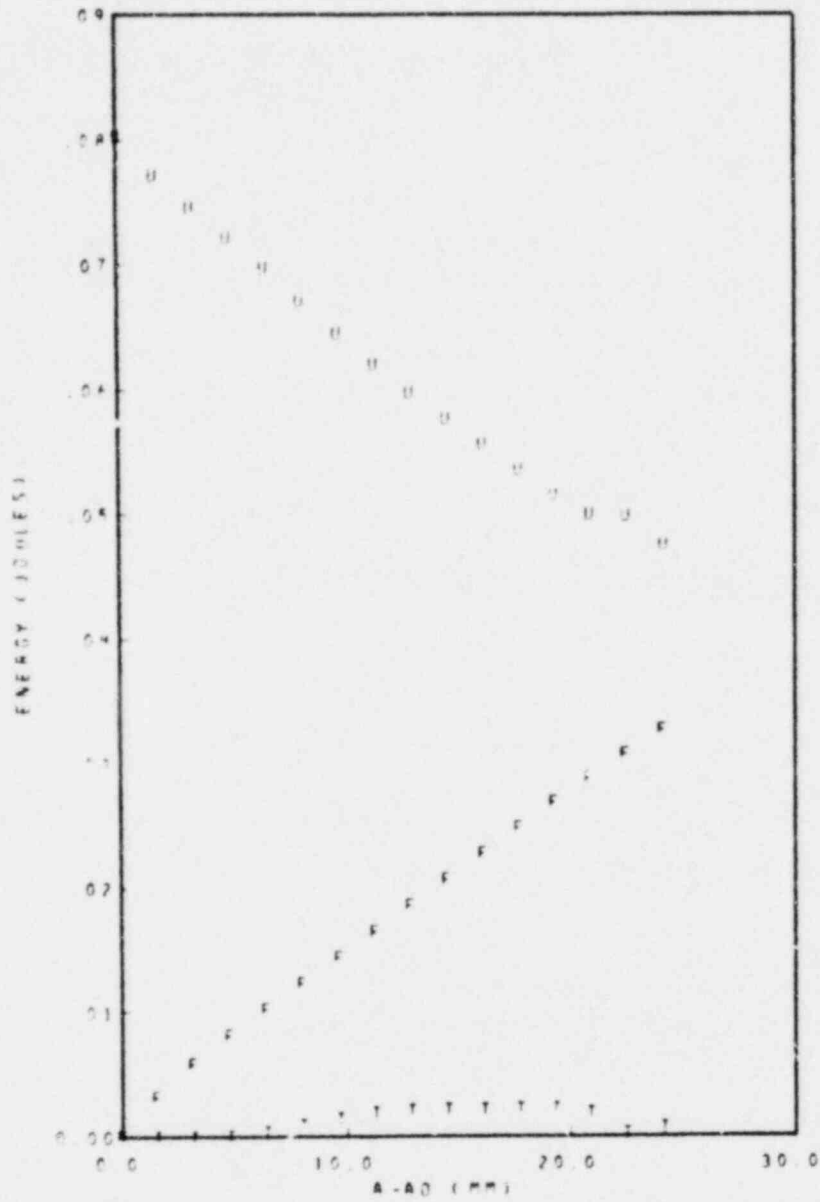


FIGURE 2.6. MODEL CALCULATIONS OF CRACK GROWTH VERSUS TIME AND ENERGIES VERSUS CRACK GROWTH IN WEDGE LOADED RECTANGULAR DCB SPECIMENS OF ARALDITE B

b. $K_{I0} = 1.04$ (nominal), pin displacement 0.245 mm dynamic elastic properties used. Variation in energy components with crack length.

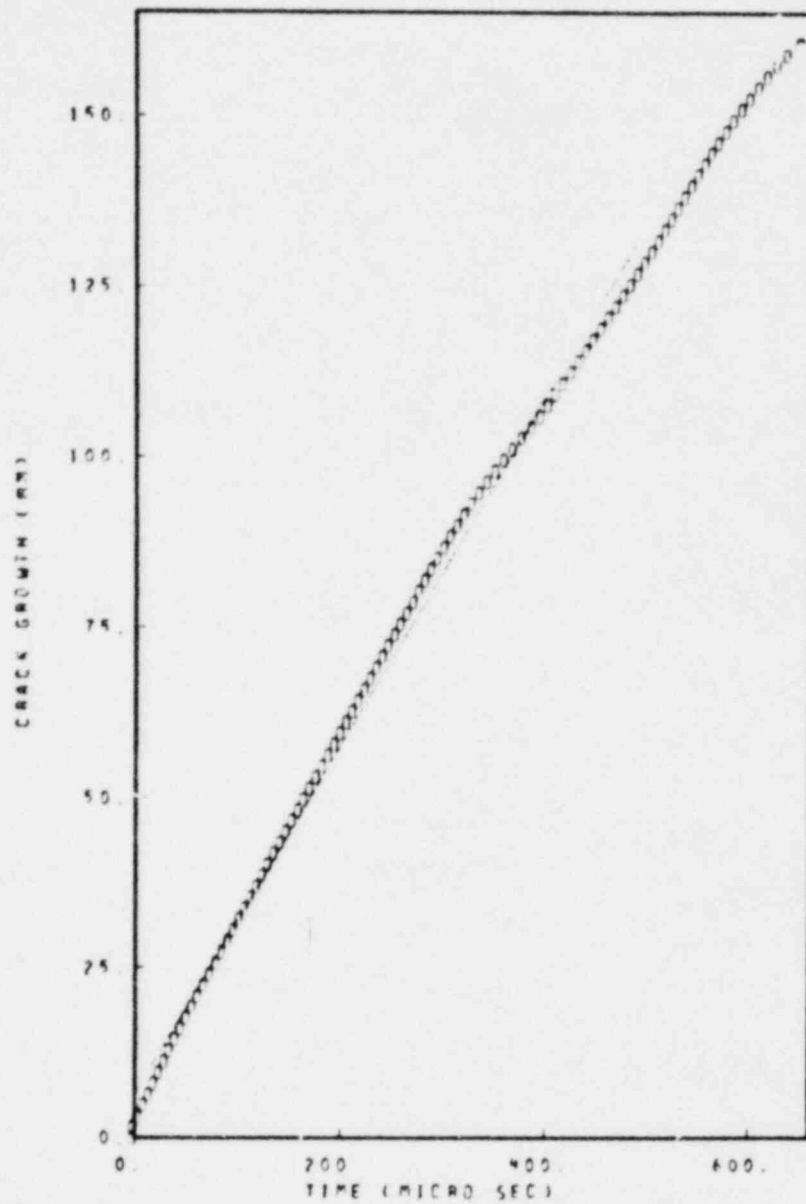


FIGURE 2.6. MODEL CALCULATIONS OF CRACK GROWTH VERSUS TIME AND ENERGIES VERSUS CRACK GROWTH IN WEDGE LOADED RECTANGULAR DCB SPECIMEN OF ALADITE B

- c. $K_Q = 2.35$ (nominal), pin displacement 0.56 mm, dynamic elastic properties used. Crack extension with time.

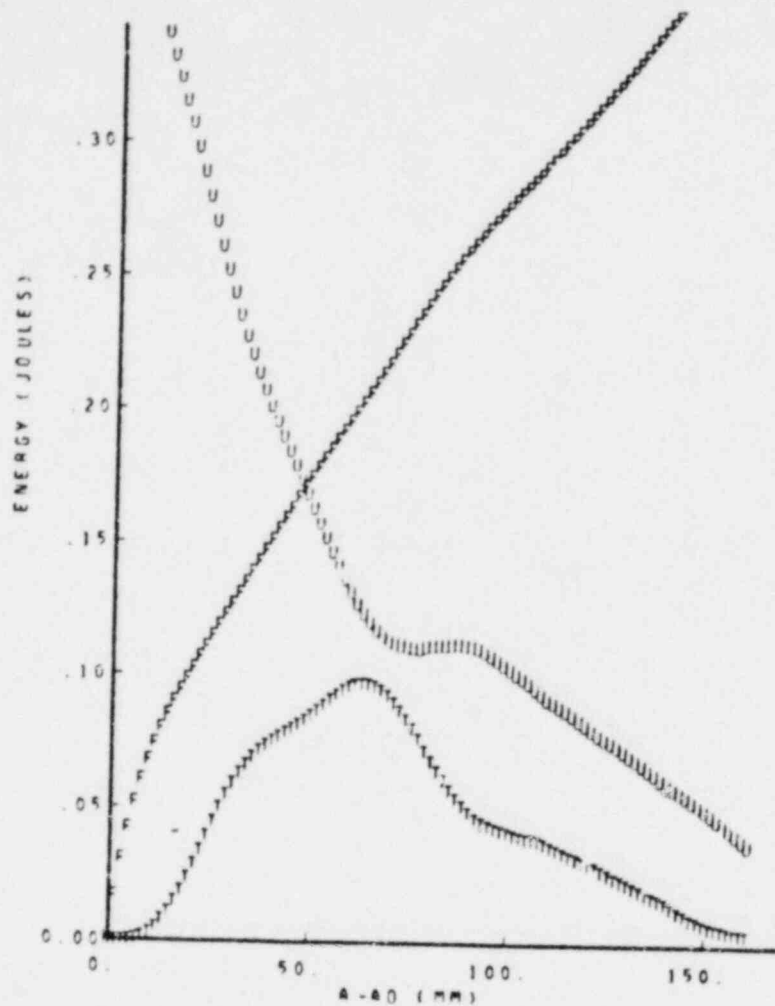
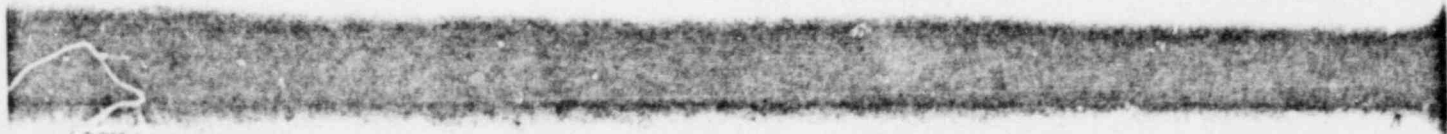


FIGURE 2.6. MODEL CALCULATIONS OF CRACK GROWTH VERSUS TIME AND ENERGIES VERSUS CRACK GROWTH IN WEDGL. LOADED RECTANGULAR DCB SPECIMEN OR ARLDITE B

- d. $K_Q = 2.35$ (nominal), pin displacement 0.56 mm, dynamic elastic properties used. Variation in energy components with crack length.



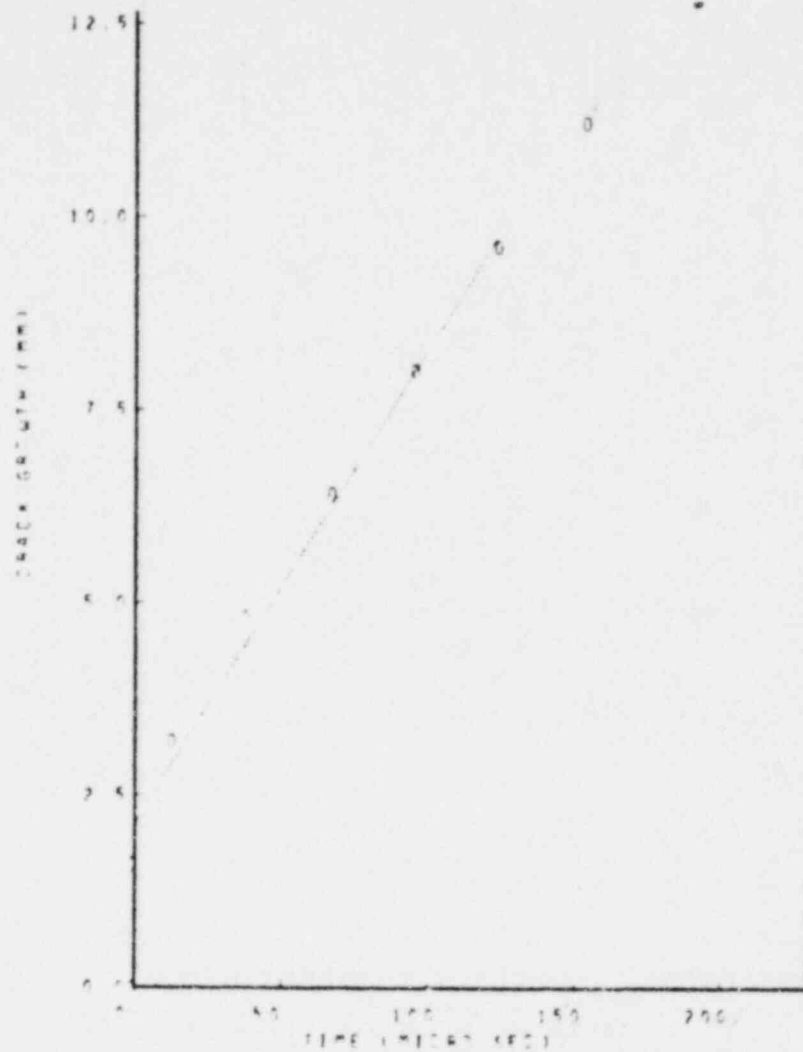
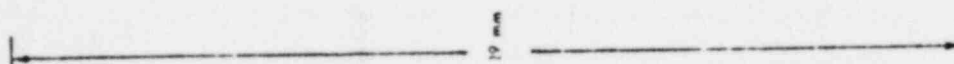


FIGURE 2.6. MODEL CALCULATIONS OF CRACK GROWTH VERSUS TIME AND ENERGIES VERSUS CRACK GROWTH IN WEDGE LOADED RECTANGULAR DCB SPECIMEN OR ARLDITE B

e. $K_{I0} = 1.04$ (nominal), pin displacement 0.245 mm static elastic properties used. Crack extension with time.



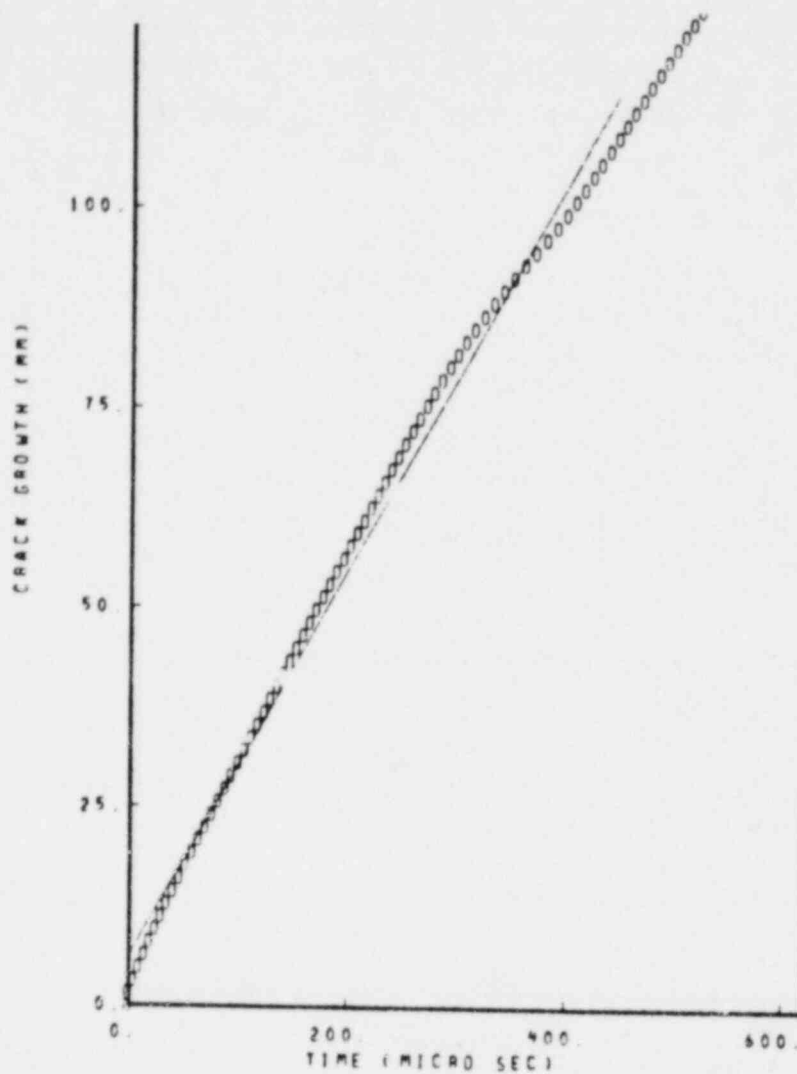
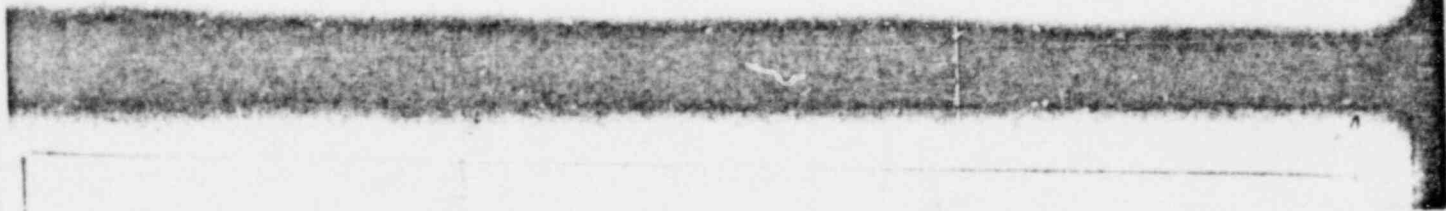


FIGURE 2.6. MODEL CALCULATIONS OF CRACK GROWTH VERSUS TIME AND ENERGIES VERSUS CRACK GROWTH IN WEDGE LOADED RECTANGULAR DCB SPECIMEN OF ARALDITE B

- g. $K_Q = 2.35$ (nominal), pin displacement 0.56 mm, static elastic properties used. Crack extension with time.



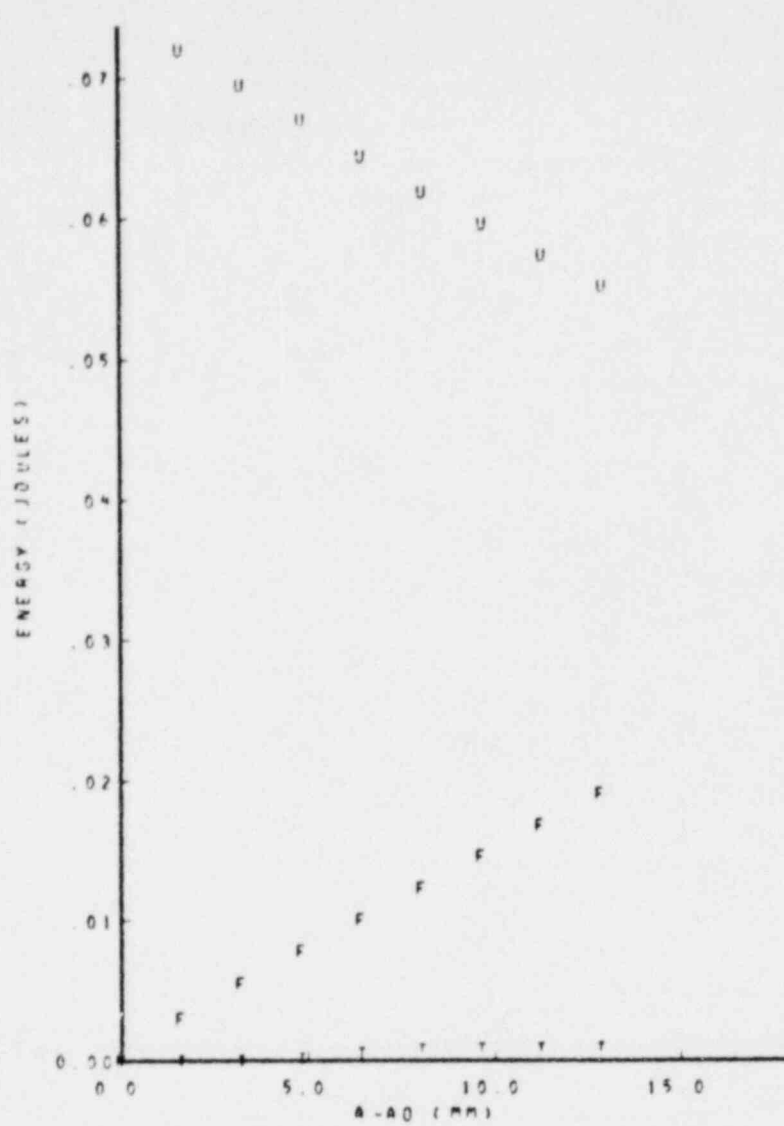


FIGURE 2.6. MODEL CALCULATIONS OF CRACK GROWTH VERSUS TIME AND ENERGIES VERSUS CRACK GROWTH IN WEDGE LOADED RECTANGULAR DCB SPECIMEN OF ARALDITE B

f. $K_Q = 1.04$ (nominal), pin displacement 0.245 mm static elastic properties used. Variation in energy components with crack length.

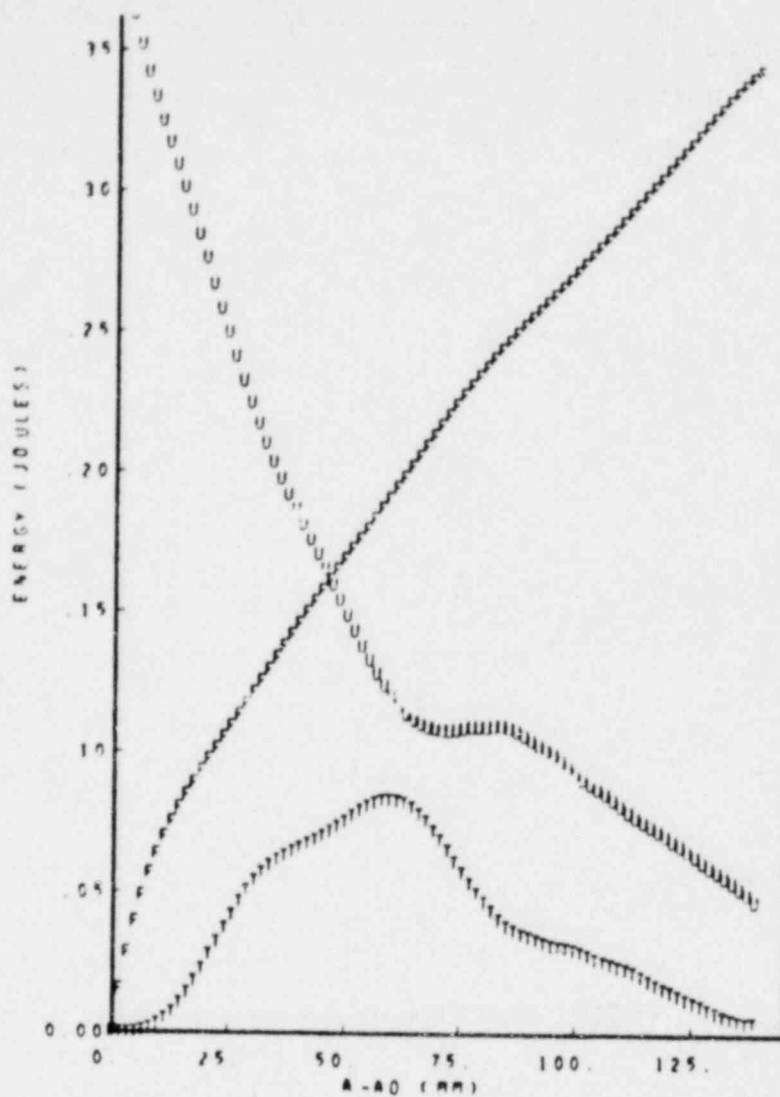


FIGURE 2.6. MODEL CALCULATIONS OF CRACK GROWTH VERSUS TIME AND ENERGIES VERSUS CRACK GROWTH IN WEDGE LOADED RECTANGULAR DCB SPECIMEN OR ARLDITE B

h. $K_Q = 2.35$ (nominal), pin displacement 0.56 mm, static elastic properties used. Variation in energy components with crack length.

mentally measured compliance of a DCB specimen somewhat more accurately than the model with torsional springs as can be seen in Figure 2.7.

Finally, in Figure 2.5 the results obtained using the static elastic properties are shown as dotted lines (...) for $K_Q = 1.04$ and $2.35 \text{ MN/m}^{3/2}$. These results, particularly those at $K_Q = 1.04$ are in poor agreement with experimental observation and obviously, this version of the model should not be used. The large discrepancy between the models using the static and dynamic elastic properties is surprising in view of the fact that there is little difference between E_D and E_S (see Table 2.1). Similar results were however observed for the polymer PMMA on another program. These results are compared in Figure 2.8 showing that the experimental data is well produced by a model using the dynamic modulus, but not by a model using a static modulus. The reason for this behavior is at present not clearly understood.

2.3. Comparison of One- and Two-dimensional Analysis

The two-dimensional analysis has been completed and successfully applied to several SEN and CT specimens (see Second Annual and Eighth Quarterly Progress Reports, BMI-NUREG-1959; 1976, and BMI-NUREG-1966; 1977). As a result of extraneous energy stored in the pins and wedge the experimentally observed crack speed versus time results cannot be unambiguously related to a well defined value of K_Q . Therefore a one-to-one comparison between the dynamic aspects of the model and experimental observation is at present not possible.

The two-dimensional analysis reproduces the experimental compliance of SEN specimens with great accuracy. For a comparison with the experimental data generated by Van den Boogaart (1966), see Figure 2.4 in Second Annual Report, BMI-NUREG-1959; 1976. Preliminary results indicate that excellent agreement is also obtained with the compliance of CT specimens measured at Battelle. In all cases tested (SEN, CT, and DCB) the strain energy release rate, \mathcal{D} , based on the model compliance and its first derivative with respect to crack length is in excellent agreement with experimental observation. However, when \mathcal{D} is evaluated from the

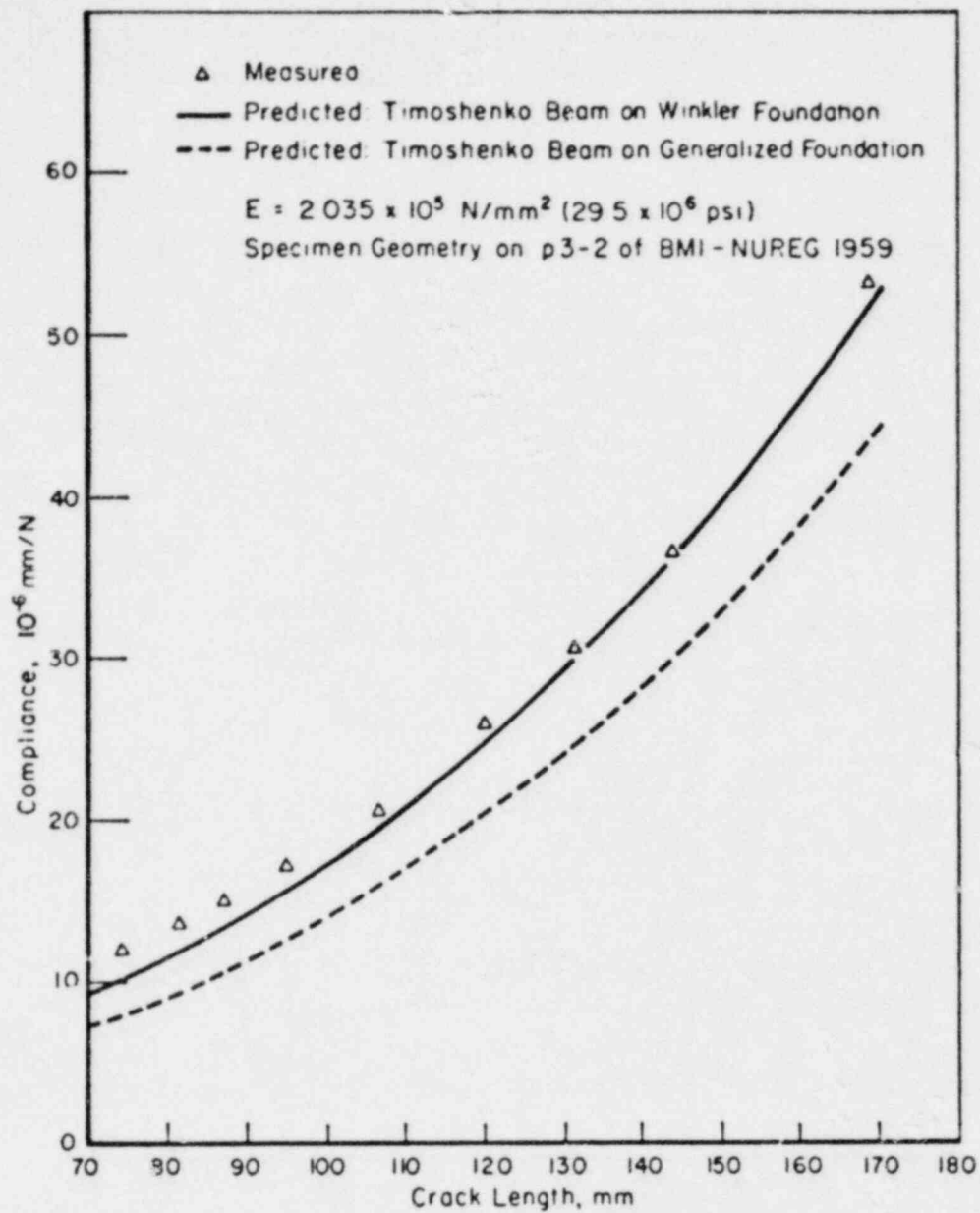


FIGURE 2.7. COMPARISON OF MEASURED AND PREDICTED COMPLIANCES

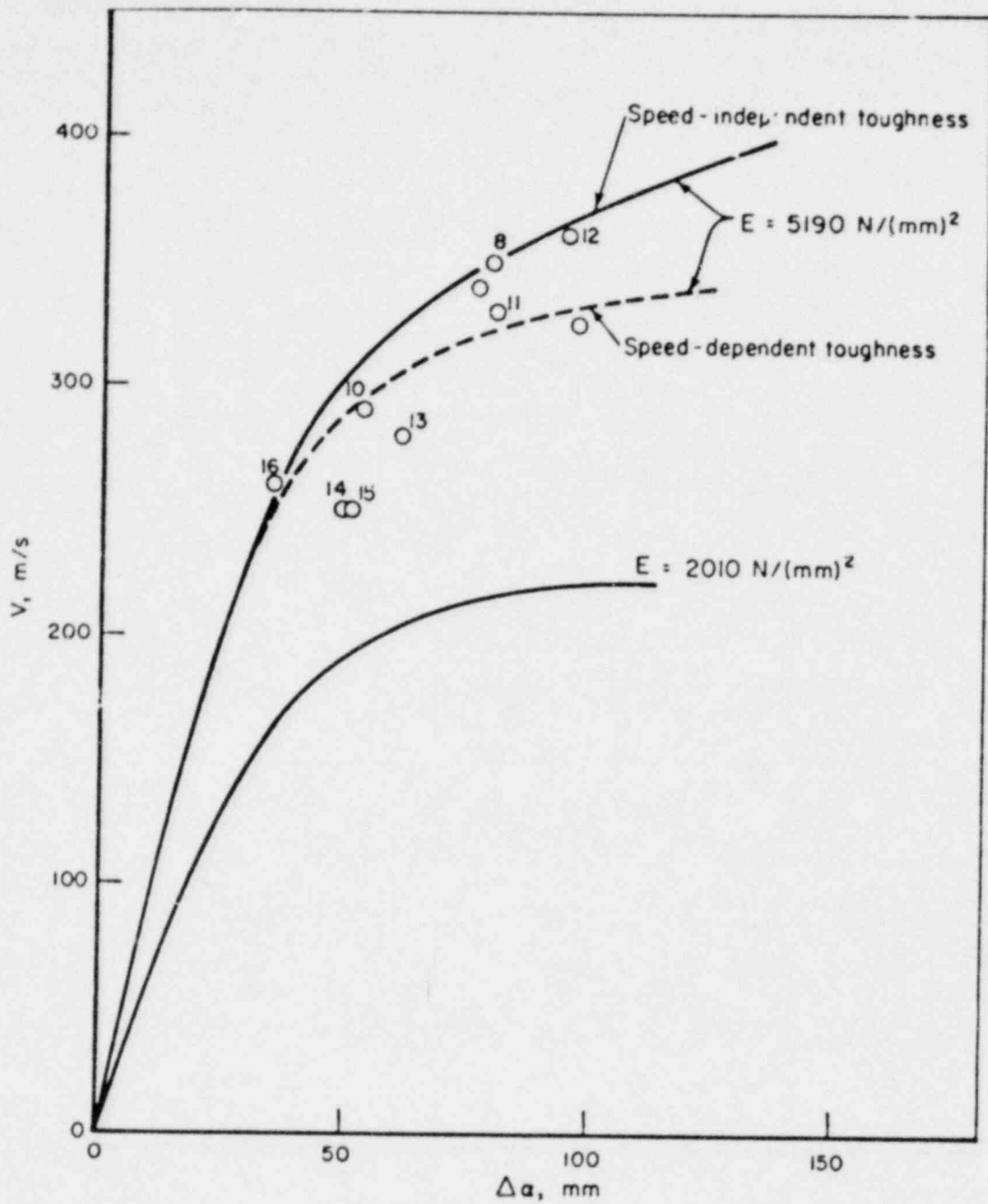


FIGURE 2.8. CRACK SPEED VERSUS CRACK GROWTH IN PMMA
 The lower solid curve is related to a model using the static modulus, while the upper two curves use the dynamic modulus. Experimental data are represented by open circles.

ment with experiment is acceptable only when the aspect ratio^{*} is less than 0.1. Since after the onset of the dynamic event u must be obtained from nodal displacements, it is important that this quantity be computed accurately.

For SEN specimens small aspect ratios can easily be achieved without having excessively small nodal spacings parallel to the crack plane. In DCB specimens however Δy is inherently small and the number of nodes parallel to the crack plane must be increased to maintain a suitably small aspect ratio. With the geometric properties given in Table 2.1, 420 nodes had to be used parallel to the crack plane (versus 8 in the direction perpendicular to that plane) to yield an aspect ratio of 0.048. In an SEN specimen a similar aspect ratio could be achieved with approximately one-quarter as many nodes. Furthermore, since in the DCB case the actual nodal spacing parallel to the crack plane is about 2.5 times smaller than in the SEN case, stability of the numerical scheme requires time steps proportionally smaller. Thus, to simulate an event of the same overall length, requires approximately $4 \times 2.5 = 10$ times more computer time in the DCB case than in the SEN case.

Despite this very large increase in computer time, it was felt that at least one two-dimensional run should be made for a DCB specimen, the reasons being as follows:

- (1) The two-dimensional analysis is inherently a more sophisticated model than the one-dimensional analysis. Since fewer assumptions have to be made, the two-dimensional model may essentially be used to validate the one-dimensional analysis. This validation is particularly important since the one-dimensional model requires less than 5% of the computer time required by the two-dimensional analysis. It also requires considerably less input preparation.

^{*}The aspect ratio is the ratio of Δx , the spacing between nodes in a direction parallel to the crack plane, and Δy , the nodal spacing in a direction perpendicular to that plane.

- (ii) The experimental data available for DCB specimens, appear to be much less subject to interpretation than data on SEN and CT specimens.

For these reasons Kalthoff's experiment on Araldite B with $K_Q = 1.34 \text{ MN/m}^{3/2}$ was analyzed. As was the case with the original one-dimensional calculations, the static elastic properties were used throughout the calculation, except in the relationship between K_D and R , where the dynamic properties were used. In the two-dimensional analysis, no point forces are used at the crack tip. The K_D versus crack speed relation is that shown in Figure 2.1

The crack growth versus time and energy versus crack extension curves are shown in Figure 2.9a and b. The two figures compare very favorably to the one-dimensional results shown in Figures 2.11d and e of the Second Annual Progress Report, EMI-NUREG-1959, 1976.

In Figure 2.10 a comparison of measured and calculated K_D and crack speeds versus crack extension is given. For comparison the original one-dimensional computations have also been included.

Although the two-dimensional model predicts an arrest length that is closer to the experimentally observed one, it is clear that both analyses predict results that are probably within the experimental error. Since neither analysis accounts for damping and since the experimental K_D versus velocity relation is known only to within $\pm 15\%$ both computed results could be modified to give a better fit yet to the experimental data. Such adjustments would have to be made on an intuitive basis and at present we feel that both models give results close to experimental observation.

The good agreement between the two models further justifies the use of the more economical one-dimensional in all studies in DCB specimens.

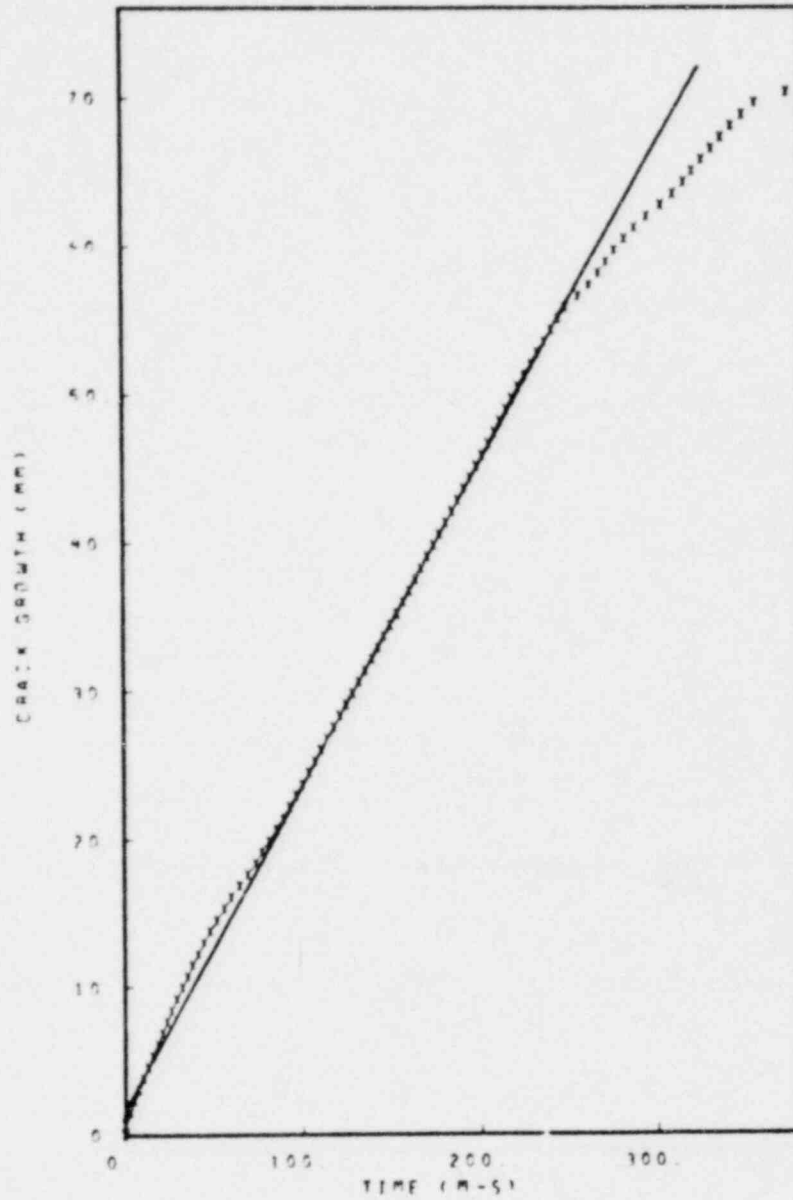


FIGURE 2.9. CALCULATED FRACTURE EVENT IN A DCB SPECIMEN OF ARALDITE B USING THE TWO-DIMENSIONAL MODEL

a. Crack growth versus time.

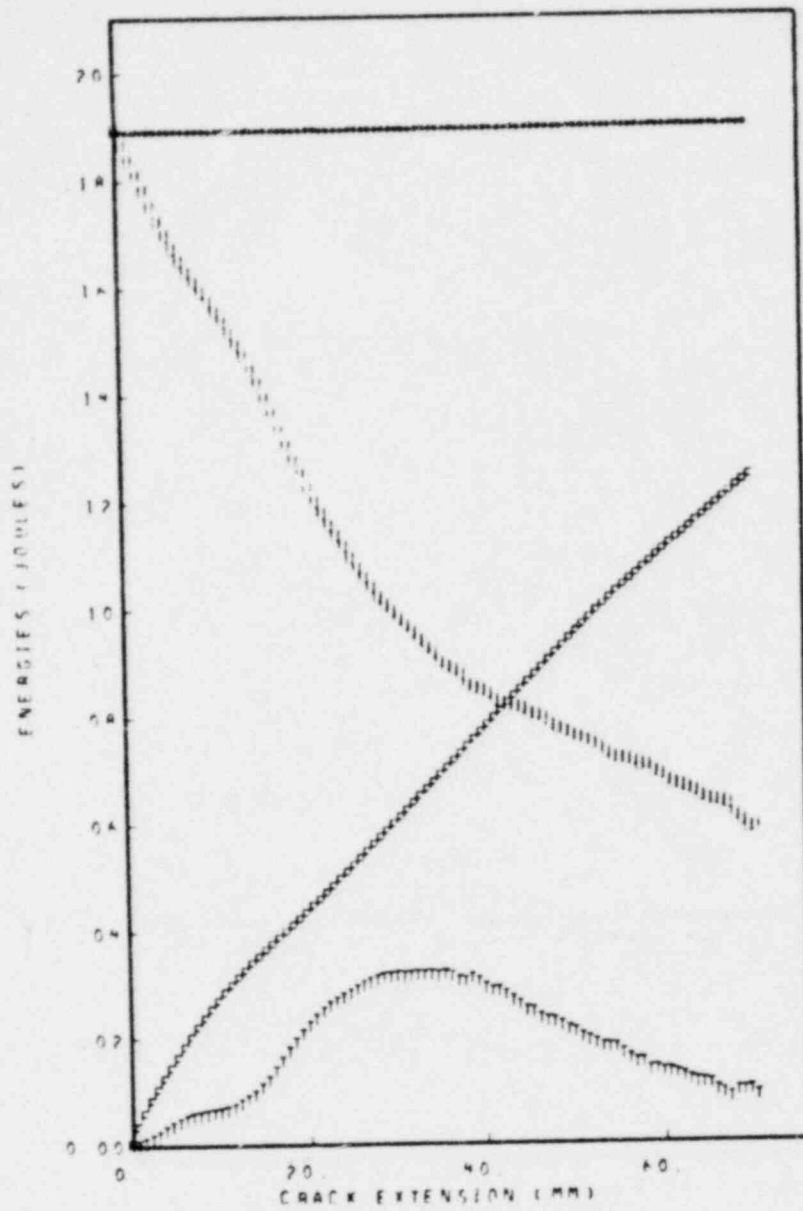


FIGURE 2.9. CALCULATED FRACTURE EVENT IN A DCB SPECIMEN OF ARALDITE B USING THE TWO-DIMENSIONAL MODEL

- b. Computation of strain (V), kinetic (T), and fracture (F) energies versus crack extension. The total energy is represented by asterisks (*). As can be seen the energy remains constant throughout the model calculation.

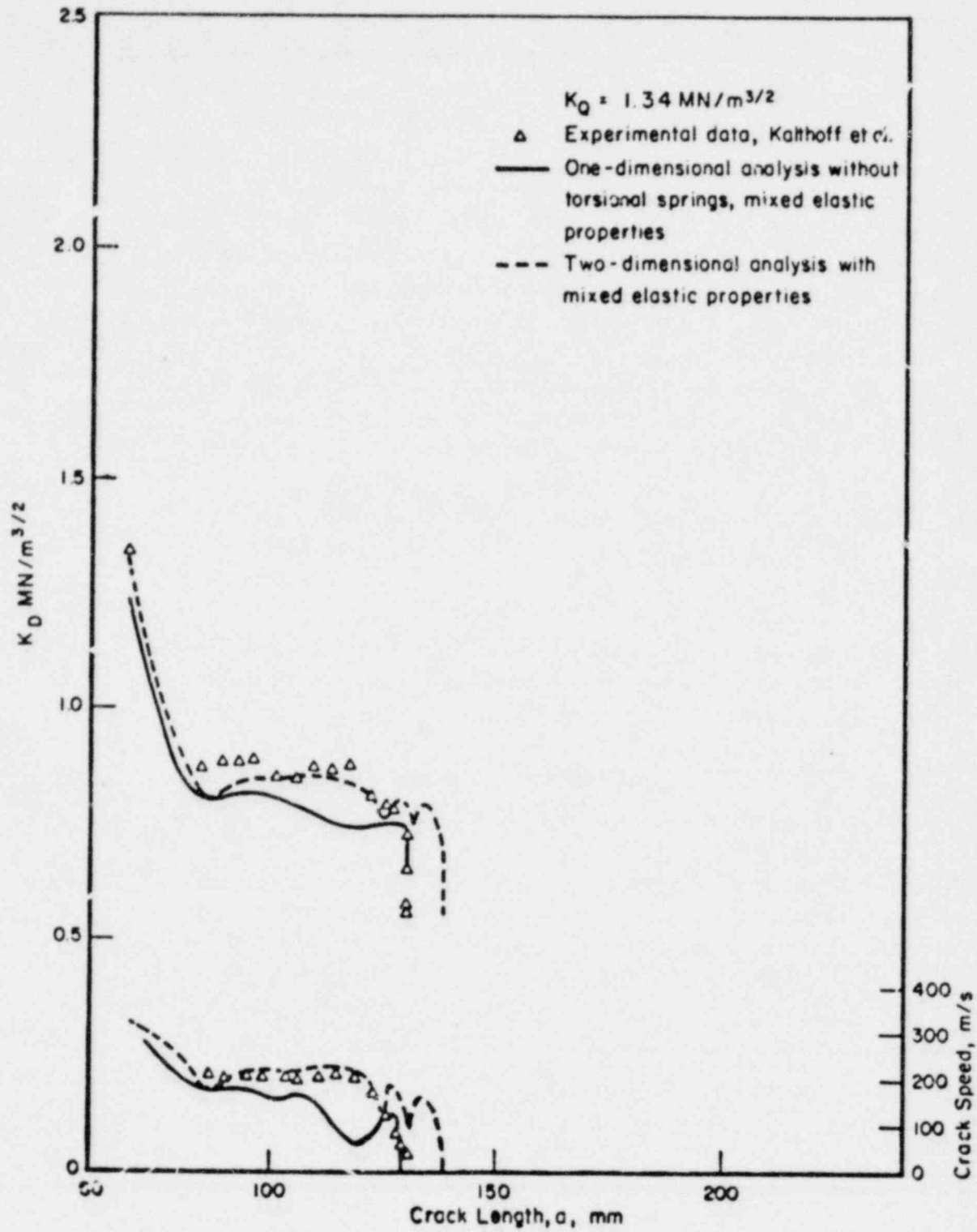


FIGURE 2.10. COMPARISON OF EXPERIMENTAL AND ONE- AND TWO-DIMENSIONAL CALCULATED RESULTS FOR ARALDITE B

3. APPLICATION OF THE COMPACT TENSION SPECIMEN GEOMETRY TO CRACK ARREST MEASUREMENTS - PRELIMINARY RESULTS

3.1. Introduction

A series of experiments are in progress to investigate the use of so-called "two-dimensional" test specimen geometries for measuring crack arrest properties. These experiments seek to:

- Minimize macrobranching which occurs in A533B steel when tested in the DCB configuration without deep side grooves.
- Provide an alternative test geometry to the DCB specimen for measuring crack arrest properties.
- Check the two-dimensional dynamic fracture analysis developed at Battelle.

In the previous report in this program (BMI-NUREG-1966, 1977) a series of experiments on a single-edge-notch (SEN) geometry was described and analyzed. These experiments involved measurements of crack velocity and total crack propagation distances in both ordinary and duplex (4340/A533B) configurations. The crack propagation events were compared with the predictions of the model and the agreement was found to be rather poor. These results pointed to several shortcomings in the specimen design and loading configuration. The major problem appeared to be lack of adequate stiffness in the load train relative to the stiffness of the specimen itself. As a consequence, the loading system does work on the specimen during crack propagation causing a larger crack extension than would be predicted using the assumption of zero interaction between the specimen and loading train.

3.2. Experimental Results

The suspicion that the stiffness of the wedge-loading arrangement was not adequate in the SEN experiments has been confirmed. The major portion of the compliance of the loading system is due to the bending of the

amount of the elastic energy available to extend the crack is contained in the loading pins. This condition is a consequence of the relatively low compliance of the SEN geometry. In previous tests on the DCB geometry, externally stored strain energy was not a problem simply because the compliance of the DCB specimen is about five times larger than the SEN specimen for the same thickness.

In an attempt to reduce the test specimen-loading machine interaction, work has been initiated with the compact-tension (CT) geometry. Three CT specimens with a gross thickness of 25 mm and side grooved 25 percent ($B_n/B = 0.75$) were machined from SEN specimens and have the design shown in Figure 3.1. The specimen is somewhat more compliant than the SEN geometry, and, in addition the loading pins have been stiffened by increasing their diameter from 31.75 mm to 44.45 mm. The three CT specimens had a duplex 4340/A533B configuration and were tested at about NDT (-12°C) by wedge loading in the tiedown fixture.

The crack length-time records for each of the three tests are shown in Figure 3.2. These records show the crack velocity to be relatively constant and, indeed, much more constant than was found in the SEN experiments.

Measurements of specimen motion in-plane were also made during the run-arrest event in tests on specimens DA-43 and DA-44. These measurements were obtained from two proximity detectors monitoring the in-plane, opening motion of the edges at points marked by "A" in Figure 3.1. The sum of the two signals from the transducers are superposed on the crack length-time graphs for specimens DA-43 and DA-44.

The displacement measurements show that the opening of the specimen initiates fairly quickly after onset of fracture. A maximum opening displacement of about 0.5 mm is reached approximately 300 microseconds after initiation. This opening occurs about 100 microseconds after arrest. Actually the specimens continue to open but at a much slower rate. This is apparent from transducer data spanning a 10 msec time interval for specimen DA-43 shown in Figure 3.3. Note that after 10 msec the crack opening has increased by about 0.8 mm. The final opening

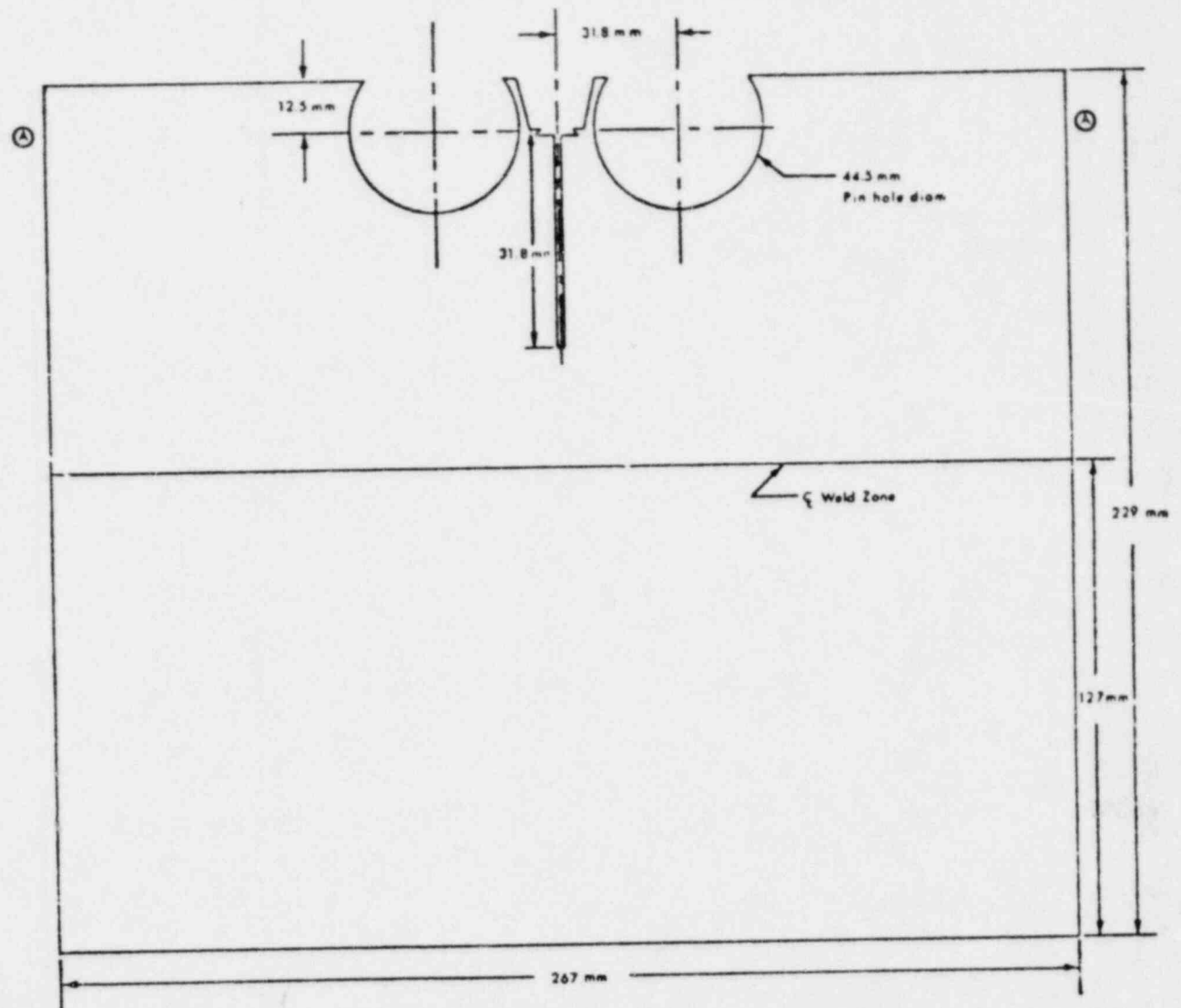


FIGURE 3.1. DUPLEX COMPACT-TENSION SPECIMEN EMPLOYED IN THE EXPERIMENTS DESCRIBED IN THE TEXT. The specimen thickness is 25.4 mm and 45° side-grooves (not shown) are machined to a depth of 3.18 mm each along the crack path. Displacement transducers were used to monitor the motion of the specimen edges during the tests at the locations identified by the circled "A".

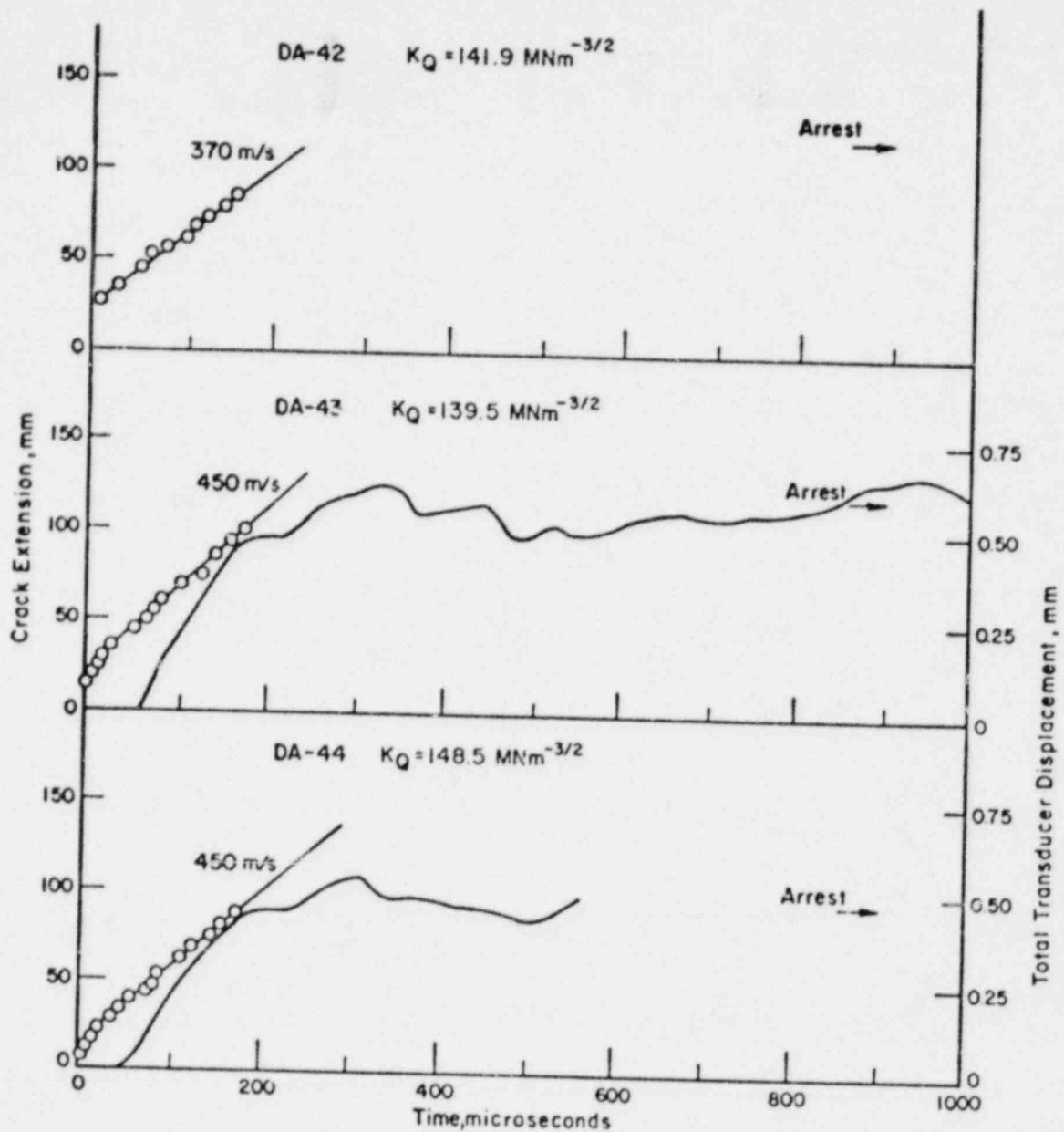


FIGURE 3.2. CRACK EXTENSION - TIME AND DISPLACEMENT - TIME RECORDS FOR THREE CT CRACK PROPAGATION EXPERIMENTS
 The tests were conducted at about -12°C and the applied stress intensity at crack initiation, K_Q , is identified for each of the three specimens. Open points identify crack position and the solid lines the total displacement recorded from transducers.

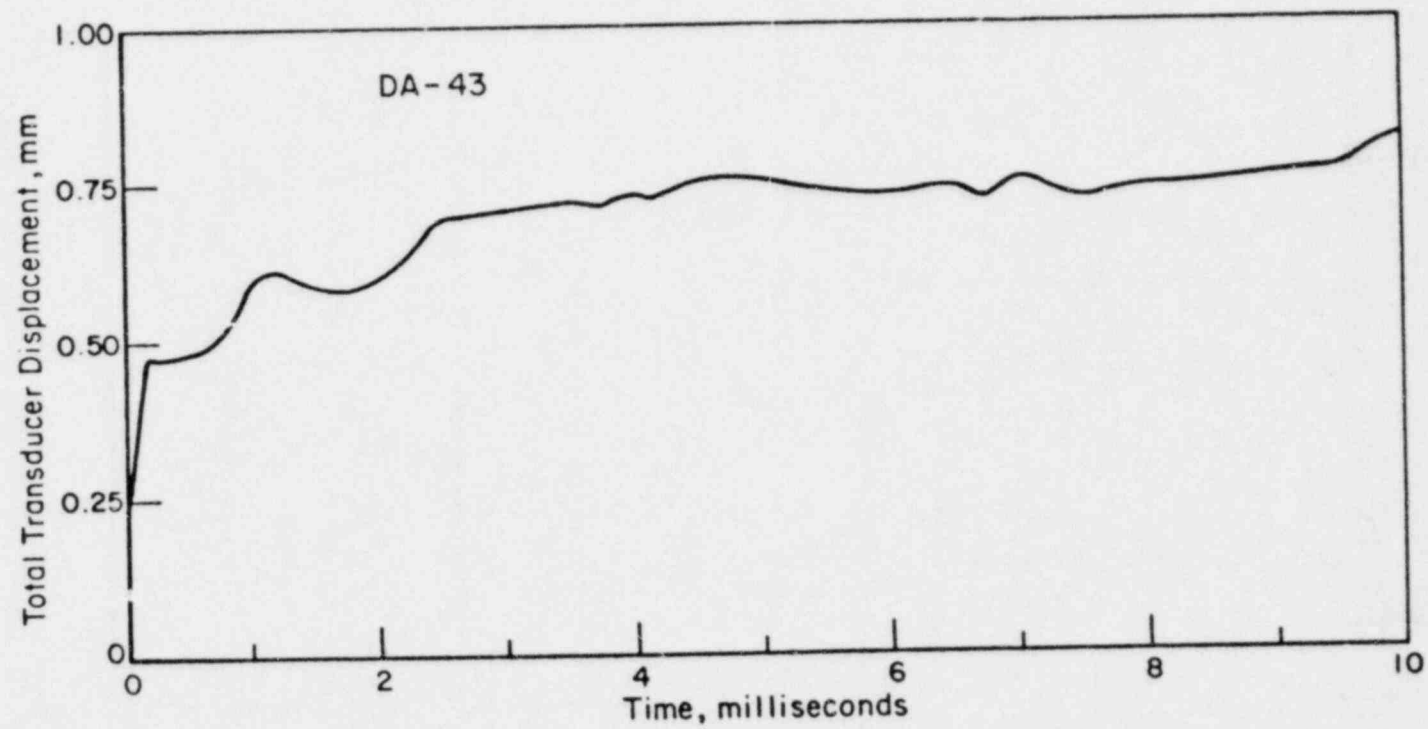


FIGURE 3.3. TOTAL TRANSDUCER DISPLACEMENT-TIME RECORD FROM EXPERIMENT DA-43 FOR 10 MILLISECONDS AFTER INITIATION OF FRACTURE

displacement in these tests measured well after the fracture event is complete (~ 2 seconds) is considerably larger than the displacement at initiation as shown in the following table. These displacements were measured by the clip gage attached to the mouth of the starter slot.

Spec.	Clip Gage Displacement (mm)		
	Initiation	Arrest	Difference
DA-42	0.74	1.75	1.01
DA-43	0.74	1.80	1.06
DA-44	0.85	1.69	0.83

Following the method outlined in BMI-NUREG-1959 (1976), the two-dimensional model can be used to evaluate the ratio K_D/K_Q from either a measurement of the relative crack propagation distance, $\Delta a/W$, or the average crack velocity \bar{V} . Table 3.1 compares the K_D values for these three tests derived by the two methods. It is evident that the K_D results obtained from $\Delta a/w$ are 20 to 30 percent below the corresponding values obtained from \bar{V} . As discussed in the next section this discrepancy could be accounted for if about 50 percent additional energy is introduced into the specimen while the crack is moving. Another important point is that a group of K_D data determined using DCB specimens taken from the same lot of A533B and tested at the same temperature was found to be $120 \pm 10 \text{ MNm}^{-3/2}$. These values agree quite well with the K_D results based on \bar{V} for the CT specimens.

A final observation of some importance is that the crack path in these tests, as in the previous SEN experiments, was relatively stable, i.e. large bifurcations were not observed. Several unbroken ligaments remained on the surfaces typical of all fractures observed in this steel after tests at -12°C .

These observations suggest the following interpretation of the fracture events. Initially the crack propagation proceeds at a velocity consistent with the fast fracture toughness, K_D , of the material and the applied K_Q level. After about 50 to 100 microseconds, the loading system

TABLE 3.1. COMPARISON OF K_D DATA FOR A533B (CBI PLATE) DETERMINED FROM CRACK PROPAGATION DISTANCE AND FROM CRACK VELOCITY IN THE COMPACT TENSION EXPERIMENTS AT -12°C

Specimen	K_Q $\text{MNm}^{-3/2}$	$\frac{\Delta a}{W}$ (a)	\bar{V} (b) m/s	(c) $K_D(\Delta a/W)$ $\text{MNm}^{-3/2}$	(d) $K_D(\bar{V})$ $\text{MNm}^{-3/2}$	K_D from DCB Tests (BMI-NUREG-1959) $\text{MNm}^{-3/2}$
DA-42	141.9	0.55	370	89.4	120.6	120 ± 10
DA-43	139.5	0.56	450	86.5	111.6	
DA-44	148.5	0.45	450	99.8	119.3	

- (a) Total crack extension distance relative to the specimen width ($W = 216$ mm).
- (b) Average crack velocity in the A533B test section.
- (c) K_D determined using the two-dimensional model and the measured $\Delta a/W$.
- (d) K_D determined using the two-dimensional model and the measured \bar{V} .

begins to open the specimen thereby increasing the total energy in the specimen. The crack velocity is apparently unaffected by this steadily increasing energy input. Instead, the crack continues to propagate at the same velocity beyond the point where arrest would have occurred. The additional crack extension is made possible by the work done on the specimen by the loading system. Arrest occurs when the rate of energy supply to the crack tip (which is now made up of contributions from both the initial strain energy in the specimen and additional work done by the load train) is insufficient to continue the fracture process. Following arrest the loading system continues to drive the opening of the specimen until equilibrium is nearly achieved. The final stage in the events is a much slower opening rate while the crack tip remains stationary. A plausible explanation of this additional opening is the expansion of the crack tip plastic zone in concert with stretching of unbroken ligaments. These deformation processes would occur under strain rate conditions which are substantially less than during propagation and therefore at reduced flow stress levels.

On comparison, the externally supplied energy in the previous SEN experiments appears to be considerably larger than in the present CT tests. Indeed cracks propagated relatively long distances in the test sections of SEN duplex specimens even though the K_{Ic} level should have been insufficient to permit any penetration of the test section. Thus, while it is apparent that the loading system needs to be stiffened further, the increased diameter of the loading pin together with the somewhat higher compliance of the CT specimen have afforded definite improvements. Certainly, a further increase in loading pin diameter would be useful. However, there is very recent evidence that a substantial improvement could be achieved by eliminating the strain energy stored in the Hertzian stress field at the contact lines between the wedge and pins. Efforts are continuing to decrease the load system-specimen interaction during propagation in two-dimensional specimens and we are hopeful that these interactions can be minimized. The next section provides guidelines for estimating the required loading system compliance relative to the test specimen compliance necessary to reduce the work input to tolerable levels.

In summary, these CT experiments appear promising in the sense that further increases in the stiffness of the wedge loading system would allow the experimentally simple determination of K_D from a measurement of Δa and K_Q .

4. SOURCES OF ERROR IN K_D MEASUREMENTS -
EFFECT OF EXTERNALLY SUPPLIED ENERGY
DURING PROPAGATION

The consequences of an interaction between the loading system and the test specimen have become quite apparent in recent crack propagation experiments on SEN and CT specimens. In this section an estimate is made of the errors caused by this externally supplied energy.

Suppose that the additional energy supplied the specimen during propagation is W which causes the crack to arrest at a'_a rather than a_a . Then, for that event we can write the energy balance as

$$R(a'_a - a_o) = W + \int_{a_o}^{a'_a} \mathcal{Y} da \quad (4.1)$$

The above equation incorporates the assumption of total recovery of kinetic energy. While this is not quite true there is the balancing effect that the work done on the specimen during propagation will also not be entirely utilized in the fracture process. To a good approximation (Hoagland and Rosenfield, 1974) the area under a curve of \mathcal{Y} versus a for many specimen geometries can be represented by the geometric mean; i.e.

$$\int_{a_1}^{a_2} \mathcal{Y} da = \sqrt{\mathcal{Y}_1 \mathcal{Y}_2} (a_2 - a_1) \quad (4.2)$$

So Equation 4.1 can be written as

$$R(a'_a - a_o) = W + \sqrt{\mathcal{B}_Q \mathcal{Y}_a} (a_a - a_o) + \sqrt{\mathcal{B}'_a \mathcal{Y}_a} (a'_a - a_a) \quad (4.3)$$

An additional expression which represents simply the consequence of the approximation in Equation 4.2 is

$$\sqrt{\mathcal{B}_Q \mathcal{Y}'_a} (a'_a - a_o) = \sqrt{\mathcal{B}_Q \mathcal{Y}_a} (a_a - a_o) + \sqrt{\mathcal{B}'_a \mathcal{Y}_a} (a'_a - a_a) \quad (4.4)$$

Letting Δa represent $(a_a - a_0)$, the zero-work crack jump distance, and δa , represent $(a'_a - a_a)$ the additional jump distance, we can combine Equations 4.3 and 4.4 and solve the resulting quadratic for δa . Before writing this result it is worthwhile to incorporate the results of the one-dimensional and two-dimensional model calculations. These calculations (cf. BHI-NUREG-1959, 1976) show that for the DCB and CT geometries a simple relation between Δa and K_Q/K_D exists of the form

$$\Delta a = C \left(\frac{K_Q}{K_D} \right) - 1 \quad (4.5)$$

In addition, we note that for a given test specimen and loading system the elastic energy contained in the loading system will be nearly proportional to the elastic energy stored in the specimen. As a result, the work done on the specimen during propagation will also be proportional to U_Q and may therefore be expressed as

$$W = \psi \gamma U_Q \quad (4.6)$$

where

$$\gamma = \frac{\phi}{d\phi/da}$$

ϕ is the compliance of the specimen and ψ is the fraction of elastic energy in the specimen at crack initiation that is supplied to the specimen by the loading system. In other words, if $\psi = 0$ the loading system is infinitely rigid, and if $\psi = 1$ the total energy in the specimen doubles during propagation.

Utilizing Equations 4.5 and 4.6 we arrive at the following result for δa .

$$\delta a = \left\{ [\psi \gamma - C(\sqrt{a} - a)](1 - a) + [(1 - a)^2 (C(\sqrt{a} - a) - \psi \gamma)^2 + 4C(\sqrt{a} - a)(1 - a)\psi \gamma]^{1/2} \right\} / [2a(1 - a)] \quad (4.7)$$

where a is equal to R/H_Q .

Finally we note that if the measured crack jump distance is used to determine K_D via the expression given by 4.5, the apparent K_D will be less than the true value due to the additional crack propagation, δa , according to the following.

$$\frac{K_D \text{ (apparent)}}{K_D \text{ (true)}} = \frac{C}{C + \delta a \sqrt{a}} \quad (4.8)$$

This expression together with Equation (4.7) is shown in Figure 4.1 for 10 percent, 50 percent and 100 percent additional energy introduced into the specimen from external sources during propagation. The results are expressed in terms of $K_Q/K_D = 1/\sqrt{a}$ for the DCB specimen ($C = 130$ mm) and the CT specimen ($C = 220$ mm).

This relatively simple analysis shows that work done on the specimen during propagation can have a substantial effect on a determination of K_D based on a measurement of the crack jump distance. For example, the analysis suggests that for a run-arrest event occurring while the loading system increases the total energy in the specimen by 50 percent the additional crack extension is sufficient to cause a 25 percent error in K_D . It is also interesting to note that for a given ψ , a slightly smaller error in K_D results in the CT specimen compared to the DCB. This is due to the fact that, for a given K_Q , the crack jump distance is larger in the present CT design than in the DCB. However, this is somewhat misleading because the compliance of the CT is about one-fifth that of the DCB. Consequently, at the same K_Q level the applied load on the CT and, thus, the energy stored in the loading system, will be five times greater. Finally, this analysis provides a useful guide for the design of a loading system. It shows that if the errors in K_D must not exceed about 5-10 percent, the loading system must not contribute more than about 10 percent additional energy during propagation. Therefore, a conservative rule of thumb, the compliance of the loading system, exclusive of the test specimen, would have to be no greater than, one-tenth that of the specimen. This estimate is conservative because only a fraction of the energy stored in the loading system at initiation is available to the specimen.

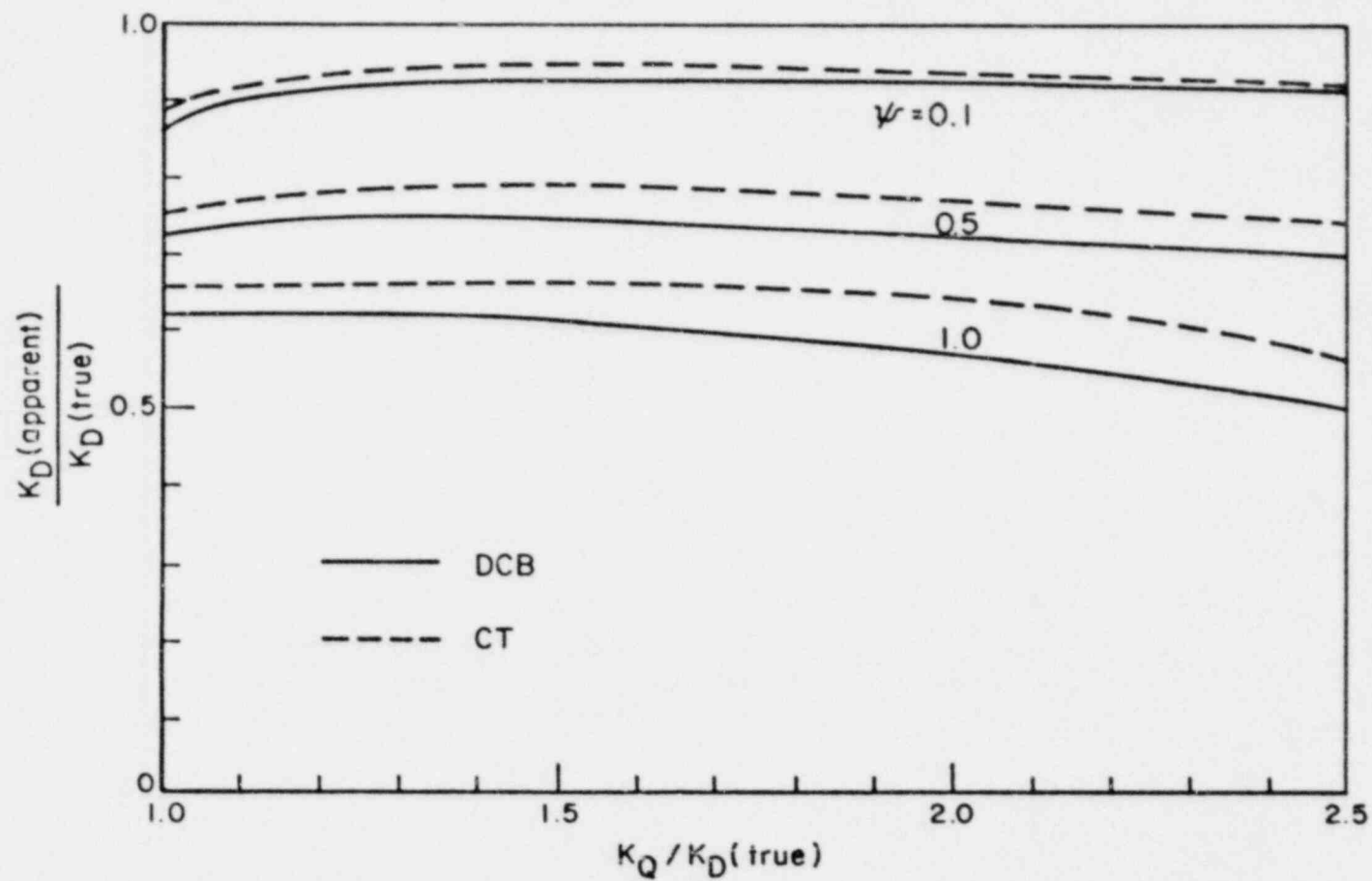


FIGURE 4.1. EFFECT OF EXTERNALLY SUPPLIED ENERGY ON THE APPARENT VALUE OF K_D DETERMINED FROM A MEASUREMENT OF CRACK PROPAGATION DISTANCE IN CT AND DCB SPECIMENS
 ψ represents the ratio of the energy supplied during propagation to the initial strain energy in the specimen at the initiation of propagation.

5. REFERENCES

Hoagland, R. G., and Rosenfield, A. R., (1974), "The Average Fracture Energy Accompanying Rapid Crack Propagation", *Int'l. J. Fracture*, 10, p. 299.

Kalthoff, J. F., Beinert, J., and Winkler, S., (1976), "Measurements of Dynamic Stress Intensity Factors for Fast Running and Arresting Cracks in DCB Specimens", *ASTM Symposium on Fast Fracture and Crack Arrest*, June 28-30, 1976.

Kobayashi, A. S., Mall, S., and Lee, M. H., (1976), "Fracture Dynamics of Wedge-Loaded DCB Specimens", to be published in *ASTM-STP*.

Van den Boogaart, A., (1966), "Crazing and Characterization of Brittle Fracture in Polymers", *Proceedings of Conference on Physical Basis of Yield and Fracture*, pp. 167-175.

ERRATA

The following photograph should have appeared as Figure 3.3 in the previous quarterly report in this series (BMI-NUREG-1966) but was accidentally omitted.

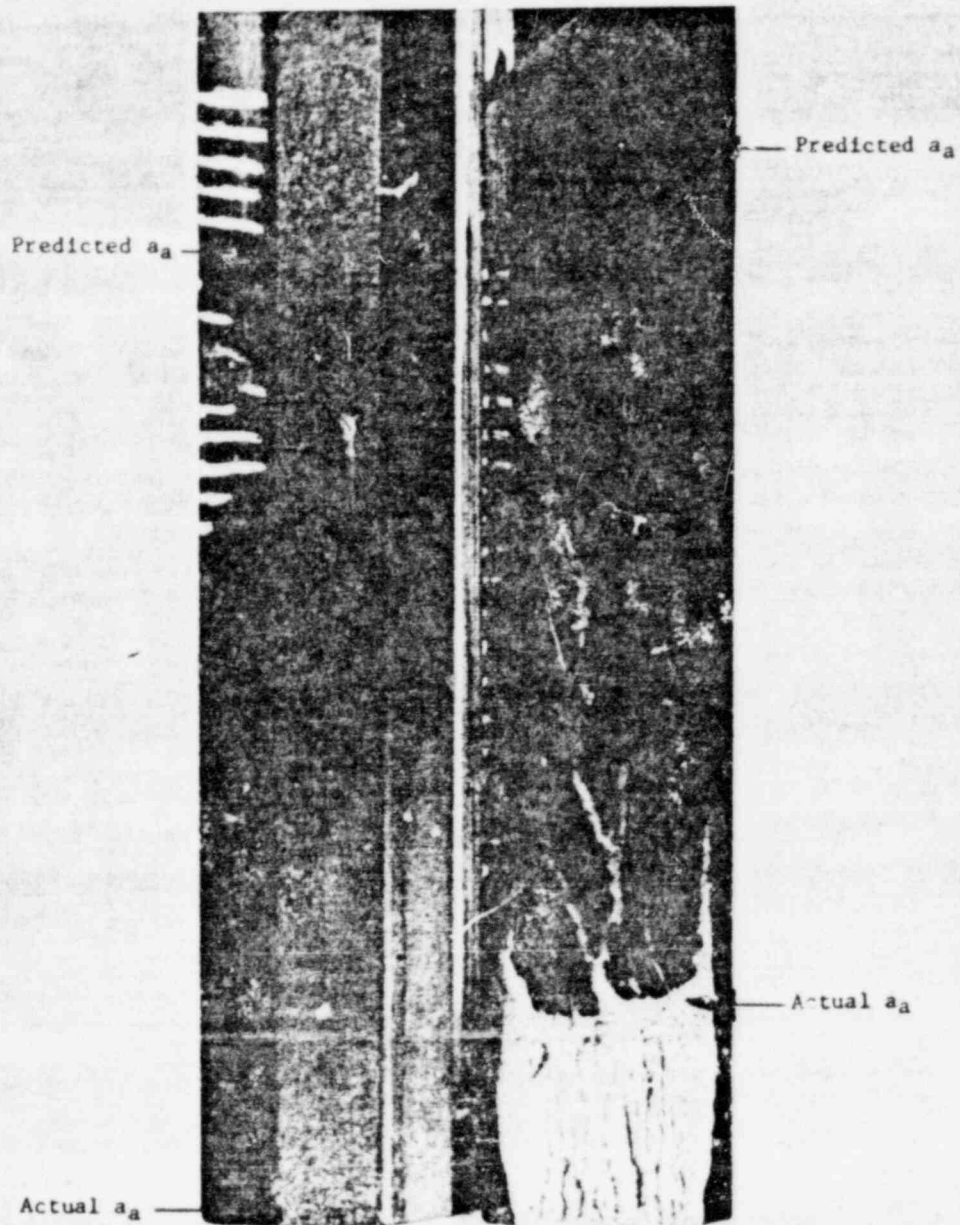


FIGURE 3.3. THE FRACTURE SURFACES OF SPECIMENS +G-3 (RIGHT) AND +G-4 (LEFT) TAPERED DCB SPECIMENS SHOWING A COMPARISON OF THE PREDICTED AND ACTUAL ARRESTED CRACK TIP LOCATIONS